IEEE Access
Multidisciplinary | Rapid Review | Open Access Journal

Received 20 August 2023, accepted 9 September 2023, date of publication 13 September 2023,
date of current version 19 September 2023.

Digital Object Identifier 10.1109/ACCESS.2023.3314742

RESEARCH ARTICLE

Harmonics Forecasting of Wind and Solar Hybrid Model Based on Deep Machine Learning

FAWAZ M. AL HADI, HAMED H. ALY, (Senior Member, IEEE), AND TIMOTHY LITTLE
Electrical and Computer Engineering Department, Dalhousie University, Halifax, NS B3H 4R2, Canada
Corresponding author: Hamed H. Aly (hamed.aly@dal.ca)

ABSTRACT Solar and Wind energy based Renewable Energy Systems (RES) are one of the most rapidly growing technologies as a means of producing clean electrical energy. Grid integration of RES involves various types of power electronics-based converters and inverters. These electronic devices produce harmonics at their terminals, which are transferred to the grid. Harmonics forecasting is one of the techniques used to design harmonics mitigation devices in order to reduce harmonics. The core objective of this work is to develop a hybrid forecasting model to produce accurate and reliable harmonics forecasts for RES. Six novel hybrid forecasting models are proposed in this work to perform harmonics forecasting. These models are based on different combinations of multi-layered Artificial Neural Networks (ANN) and Adaptive Neuro Fuzzy Inference System (ANFIS). The forecasting models proposed are two-staged architecture. Three hybrid forecasting models (model-1, 2 & 3) use ANN in the first stage and ANFIS in the second while the other three models (model-4, 5 & 6) are designed vice versa of prior. Two renewable generators are used to generate harmonics. The first generator combines Double-Fed Induction Generator (DFIG) driven by wind turbine with solar photovoltaic (PV) panels whereas, the second generator combines wind turbine driven Permanent Magnet Synchronous Generator (PMSG) with solar panels. The purpose of these generators is to produce voltage and current waveforms using real-world data (Wind Speed & Solar Irradiation). Harmonics are extracted from these waveforms which are used to create training and testing datasets for the forecasting models. Harmonics are forecasted using the six forecasting models proposed and results are validated by comparing them to benchmark work done in the literature. The results show that model-3 and model-6 are the best and most consistent performing models.

INDEX TERMS Harmonics, renewable energy systems, power quality, artificial neural networks, advanced neuro fuzzy inference system.

ABBREVIATIONS

DFIG	Double Fed Induction Generator
PMSG	Permanent Magnet Synchronous Generator
PV	Photovoltaic
RES	Renewable Energy Systems
EPS	Electrical Power System
PQ	Power Quality
PCC	Point of Common Coupling
VSC	Voltage Source Converter
THD	Total Harmonics Distortion
TDD	Total Demand Distortion
ANFIS	Adaptive Neuro Fuzzy Interference Systems
ANN	Artificial Neural Network
IEC	International Electrotechnical Commission
IEEE	Institute for Electrical and Electronics Engineers
FFT	The Fast Fourier Transform
RMSE	Root Mean Square Error
MAE	Mean Absolute Error
MLPNN	Multilayer Perceptron Neural Network (MLPNN)
NARX	Nonlinear Autoregressive with Exogenous inputs
LMS	Least Mean Square
NLMS	Normalized LMS

The associate editor coordinating the review of this manuscript and approving it for publication was Muhammad Sharif.

VLLMS	Variable Leaky Least Mean Square
UDR	Univariate Dimension Reduction
LSTM	Long Short-Term Memory
JRC	Joint Research Centre
SLP	Single Layer Perceptron
MLP	Multilayer Perceptron
RNN	Recurrent Neural Network
CNN	Cascaded Neural Network
FIS	Fuzzy Inference System
THDV	Voltage Total Harmonics Distortion
THDI	Current Total Harmonics Distortion

I. INTRODUCTION

There is a growing need for electrical energy produced from renewable energy sources, making it one of the most crucial issues to address. The increasing adoption of renewable/sustainable energy production technologies on the Electrical Power System (EPS) has given rise to novel concepts like smart grids and microgrids [1]. One of the key difficulties in achieving stability in EPS, which leads to a decline in its Power Quality (PQ), is the unpredictable and uncontrollable nature of these Renewable Energy Systems (RES) in terms of power production. With limited controllability, unfavorable power flow patterns, and non-sinusoidal current and voltage waveforms, RES differ from traditional power sources in several ways. Besides, grid integration of RES involves various types of power electronics-based converters and inverters [2]. At their terminals, these electronic devices generate both current and voltage harmonics, which are then sent to the rest of the grid [3], [4]. Harmonics can adversely affect the life of connected equipment by overheating transformers or causing malfunction in the protection systems beside other factors [5], [6]. According to IEEE 519-2014 recommendations [7] and IEC 61000 standards [8], [9], [10], harmonics are one of the most crucial features that must be kept to a minimum to ensure network power quality. Several indices, such as Total Harmonics Distortion (THD) and Total Demand Distortion (TDD), which are used for voltage and current harmonics, have been developed to measure the degree of distortions present in the original signal [11]. For instance, according to IEEE 519-2014, the voltage THD in the Point of Common Coupling (PCC) must be less than 5% limit. In order to reduce harmonics, harmonics forecasting is one of many techniques used to design harmonics mitigation devices [12], [13].

Harmonics forecasting involves predicting the future behavior of time series data that exhibits periodic patterns or harmonics. A study of literature reveals that efforts are being made to forecast harmonics as it could serve as an important input to improve power quality. One of such application is filtering which could use predicted harmonics to refine its design in order to enhance their performance. Researchers have used a variety of methods to achieve accurate prediction. The Adaptive Neuro Fuzzy Interference Systems (ANFIS) and Artificial Neural Network (ANN) are among the techniques used by authors to produce harmonics forecasts. The aim of this work is to develop and evaluate a hybrid forecasting model that effectively captures the complex harmonics patterns in time series data and provides accurate predictions. The research will focus on integrating a forecasting model that combines the strengths of ANFIS and multi-layered ANN to improve the accuracy and robustness of harmonics forecasting. The integrated ANFIS-ANN models is expected to effectively capture the complex harmonics patterns in time series data and provide accurate predictions.

II. BACKGROUND

Traditionally, utility companies used to know the precise industry of the customers who possessed the dominant harmonics sources. As a result, harmonics problems were corrected by using a passive harmonics filter at the Point of Common Coupling (PCC) of major distorting loads [14], [15], [16]. The harmonics in the power system has been observed to rise as a result of the grid integration of renewable energy sources, which uses a variety of power electronics-based converters [18], [19]. Hence, in order to determine the necessary compensation to prevent the effects produced by harmonics and to anticipate and alleviate problems brought on by their existence, utilities must be able to forecast the projected impact of harmonics. In order to maintain power quality and guarantee harmonics levels within acceptable bounds, authors in literature have tried to apply harmonics forecasting.

A harmonic forecasting method based on the Variable Leaky Least Mean Square (VLLMS) algorithm was put forth by Ray et al. in [20]. To avoid parameter drift, the suggested method employed a leak compensating technique. To speed up convergence in this process, the step size was also changed. Also, a real-time power system was simulated using several examples to show how the suggested approach is superior to other methods provided in [20]. Ivry et al. in [21] looked at how uncertainty affected harmonics prediction in a power system with many Voltage Source Converters (VSCs). The level of harmonics distortion of the VSCs observed at the PCC to the grid was predicted using the Univariate Dimension Reduction (UDR) approach. The proposed prediction approach ensured complete interactions between the harmonics sources (VSCs) and the entire power system for predicting the THD at the PCC. Hussam et al. in [22] developed the idea of adaptive filters that use real-time harmonics prediction algorithms by adopting the Least Mean Square (LMS), Normalized LMS (NLMS), and Recursive Least Square (RLS) approaches. To further reduce the time delay caused by the harmonic information collecting process, this was used in an active filter.

Based on information from a limited number of smart meters, Rodríguez-Pajarón et al. in [23] presented an approach for estimating voltage THD for Low Voltage busbars of residential distribution feeders. Various voltage THD forecasting methods, including feed-forward and autoregressive Artificial Neural Networks (ANN), were used. With this

method, new capabilities can be added to existing monitoring tools to predict harmonics distortion in the future. A network of advanced smart meters with a small number of these meters was shown to be sufficient for precise harmonics estimations [23]. In addition, Mori and Suga in [24] suggested a technique for forecasting power system harmonics voltages based on artificial neural networks (ANN). Recurrent neural networks were used to manage harmonics dynamics (RNN). Four RNNs, notably the Jordan, Elman, Noda, and Nagao models as well as a fourth model that included a context layer between the output and hidden layers as a separate recurrent network, were used to forecast the fifth harmonics voltage. It was discovered that the Elman's technique outperformed the other models [24].

In order to track the impacts of the current harmonics produced by PV systems, Mori and Suga in his research [24] introduced long-term current harmonics distortion prediction models. The suggested models employ a Multilayer Perceptron Neural Network (MLPNN) to forecast current harmonics. The 10-kW PV system's PCC and the distribution network's data from a year's worth of power quality measurements, as well as meteorological information (solar irradiance and ambient temperature) gathered at the test site, were used to train the models. Six different models were built, tested, and certified, varying in the number of hidden layers and input parameters. The fifth, seventh, eleventh, and thirteenth were predicted using a three-phase, grid-connected PV plant inverter using MLPNN. The results of the MLPNN model prediction demonstrated that adding the third input parameter (time of day) to the models improved performance to a small extent [24].

Panoiu et al. in [26] presented a study on the modelling and prediction of total harmonics distortion of current emerging in an electric arc furnace's medium voltage installation. Adaptive Neuro Fuzzy Interference Systems (ANFIS) in MATLAB are used for modelling. According to the findings, ANFIS has a good understanding of how to adjust THD. As a result of the system's ability to read 800 data points, it can provide THD variation for another 400 examples with a very low error rate. It was also attempted to train the system with varying numbers of samples from all the samples. However, the system fails to model appropriately when the number of samples used in training is less than the number used in testing [26].

Shengqing et al. [27] proposed the Hybrid Active Power Filter (HAPF) harmonics current prediction methods based on Empirical Mode Decomposition (EMD) – Support Vector Regression (SVR) theory to solve the microgrid power quality problem. This strategy first explores harmonics currents for each harmonics using EMD, and then predict the next step harmonics currents of different times using SVR's varied kernel functions, and finally the predicted value of each harmonics weighted summation was determined. The simulation results demonstrated the EMD decomposition for all harmonics for harmonics current and the usage of different kernel functions in SVR to predict harmonics currents at the next step, and finally, the predicted value of each harmonics weighted summation. In conclusion, the author established that by adopting this combination of EMD-SVR the harmonics currents at the next time step could be accurately predicted, resulting in harmonics current minimum error compensation [27].

Long Short-Term Memory (LSTM) deep learning was employed by Kuyunani et al. [28]. In order to train the network, 8103 samples of voltage harmonics from the Jeffreys Bay Wind Farm in the Eastern Cape Province were used in the study. In two steps, the proposed approach collected important data from voltage harmonics signals. To determine the mean voltage amplitude, moving window segmentation was employed. Based on the retrieved voltage attributes, the prediction of voltage harmonics production using LSTM was made. The LSTM model predicted the following 3800 sample mean values with a low Root Mean Square Error (RMSE) [28].

Hatata and Eladawy [29] used Nonlinear Autoregressive with Exogenous inputs (NARX) neural network in their research in order to anticipate the load current harmonics introduced into electric power systems. The suggested technology was used on a micro grid at the Khalda – Main Razzak power station in west Egypt, which is a petroleum site. The test nonlinear load was an Electrical Submersible Pump, driven by an induction motor and controlled by a Variable Speed Drive. In their work, they explained the process for developing the suggested NARX network to simulate nonlinear loads and calculate their THD of currents. The intended network was tested using both simulated pure sinusoidal voltage waveform and standalone measured voltage with the aim of finding the actual harmonics current of the load and the nonlinearity of each load. It was found that the recommended NARX method was faster and more accurate than the Recurrent Neural Network (RNN)-based strategy by contrasting it with the latter [29].

Pang [30], in their study, developed a method of Stack Auto Encoder (SAE) Neural Network-based short-term harmonics forecasting and evaluation affected by electrified trains on the power grid. The goal of harmonics forecasting was achieved by the findings, and the harmonics value was assessed using the techniques of harmonics assessment. It offers a theoretical frame of reference for the harmonics analysis of the impact of the railroad, which can help enhance the power quality in the power network.

Hamed [31], in his study offers a statistical framework for examining modal behaviour, trend extraction, and forecasting based on Dynamic Harmonics Regression (DHR). Synthetic and observational data were both used to evaluate the model's performance. Wind power generation measurements were used to test the practical applicability of this technique under diverse data gathering settings. The forecasting function of the DHR model, was shown to be a useful tool which could compete with other techniques already in use, exhibiting a

low error in forecasting data that can be decreased by an appropriate selection of the moving window.

A summary of literature review discussed is presented in Table 1 describing the strengths and weaknesses of the forecasting models discussed. In continuation of the literature review presented, the core objective of this work is to develop a forecasting model for accurate and reliable harmonics forecasting. To achieve this, six hybrid forecasting models are proposed, which are constructed by a combination of Artificial Neural Network (ANN) structures and Advanced Neuro Fuzzy Inference System (ANFIS). As a first step, two hybrid generator models are utilized to produce current and voltage harmonics. The first hybrid model is based on using a Doubly Fed Induction Generator (DFIG) driven via a wind turbine with Photovoltaic panels (Wind DFIG-PV). The other model is a hybrid of wind and photovoltaic using Permanent Magnet Synchronous Generator (PMSG). After getting output waveforms, harmonics are extracted from the data which forms datasets for training and predicting harmonics by using the proposed forecasting models. Furthermore, following section provide rationale to construct hybrid models by combining ANN and ANFIS models for this work.

III. RATIONALE TO BUILD HYBRID MODEL COMBINING MULTILAYERED-ANN WITH ANFIS FOR HARMONICS FORECASTING

Harmonics forecasting is an important task in various fields most importantly in improvement of power quality and grid integration of renewable energy generators. The objective is to predict the behaviour of harmonics components to serve as inputs for RES integration to the grid. To improve the accuracy and reliability of harmonics forecasting, a hybrid model that combines multilayered artificial neural networks (ANN) with adaptive neuro-fuzzy inference systems (ANFIS) can be considered. This approach offers several benefits and provides a robust solution to harmonics forecasting problems. The rationales behind building such a hybrid model is discussed as follows:

A. COMPLEMENTARY STRENGTHS OF ANN AND ANFIS

Artificial neural networks (ANNs) are powerful computational models capable of learning complex nonlinear relationships between inputs and outputs. They excel at recognizing patterns and capturing hidden dependencies in the data. ANNs can efficiently handle large volumes of training data and can generalize well to make predictions on unseen data. On the other hand, ANFIS combine the strengths of fuzzy logic and neural networks. They can model fuzzy rules, linguistic variables, and expert knowledge to provide transparent and interpretable results. ANFIS can handle uncertain and imprecise data effectively and capture the nonlinear relationships present in the data. Combination of ANNs and ANFIS in a hybrid model can benefit from the complementary strengths of both techniques. ANNs can handle complex patterns and capture intricate nonlinear relationships, while ANFIS can incorporate expert knowledge and provide interpretable results.

B. CAPTURING NONLINEARITIES AND COMPLEX RELATIONSHIPS

Harmonics forecasting often involves dealing with nonlinearities and complex relationships between harmonics components and other variables. ANNs are well-suited for capturing such nonlinear relationships due to their ability to model complex functions. By training a multilayered ANN on a dataset containing harmonics measurements and other relevant variables, ANN's capability to capture the intricate relationships between the variables and the harmonics behaviour can be exploited.

ANFIS, with its fuzzy rule-based structure, can handle linguistic variables and expert knowledge effectively. By integrating ANFIS into the hybrid model, domain expertise and fuzzy logic-based rules can be incorporated, which can enhance the forecasting accuracy by capturing the underlying linguistic patterns in the data.

C. IMPROVED FORECASTING ACCURACY AND ROBUSTNESS

The combination of ANN and ANFIS in a hybrid model can lead to improved forecasting accuracy and robustness. ANNs can learn from historical data patterns and make accurate predictions, while ANFIS can provide interpretability and handle uncertainties. The hybrid model can leverage the strength of both techniques, leading to more reliable and accurate harmonics forecasts.

D. ADAPTABILITY AND GENERALIZATION

The hybrid model can adapt to different datasets and generalize well to unseen data. ANNs are known for their ability to adapt to new patterns and data variations, enabling the model to capture changing harmonics behaviours over time. ANFIS can adapt its fuzzy rules and linguistic variables based on the input data, making the hybrid model adaptable to different operating conditions and system configurations.

E. MODEL TRANSPARENCY AND INTERPRETABILITY

The transparency and interpretability of the hybrid model are crucial in harmonics forecasting applications. ANFIS, with its fuzzy rule-based structure, provides a transparent framework that allows experts to understand and interpret the model's decision-making process. This interpretability can aid in identifying the factors contributing to harmonics variations and assessing the model's reliability.

F. SUMMARY

Table 2 presents a summary of the model components and their specific contributions to building a hybrid model based in combining multilayered ANN and ANFIS for harmonics forecasting. In conclusion, developing a hybrid model for harmonics forecasting that combines multilayered ANN and ANFIS offers several benefits. The model may incorporate

TABLE 1. Strengths and weaknesses of forecasting models.

METHOD	STRENGTHS	WEAKNESSES	REF
Variable Leaky Least Mean Square (VLLMS)	- Ability to track and adapt to changes in the underlying data distribution - Reduced sensitivity to initialization parameters	- Limited robustness against outliers or non-stationary data - Requires careful tuning of hyperparameters	[20]
Univariate Dimension Reduction (UDR)	- Capability to handle high-dimensional and correlated time series data - Effective in capturing relevant features and reducing dimensionality	- Limited interpretability compared to other methods - Complexity in determining the optimal number of principal components	[21]
Least Mean Square (LMS)	- Simplicity and ease of implementation - Low computational complexity	- Slow convergence rate, especially in non-stationary or highly correlated data - Sensitivity to step size (learning rate) selection	[22]
Recursive Least Square (RLS)	- Enhanced adaptability and faster convergence compared to LMS methods - Robustness against noise and non-stationary data	- Higher computational complexity compared to LMS methods - Sensitivity to the selection of the forgetting factor and initial covariance matrix	[22]
Artificial Neural Networks (ANN)	- Ability to capture nonlinear relationships and patterns in time series data - Flexible architecture that can handle various input features and time series characteristics	- May suffer from overfitting if not properly regularized - Prone to sensitivity in parameter initialization and network architecture design	[23], [24], [25]
Adaptive Neuro Fuzzy Interference Systems (ANFIS)	- Ability to handle nonlinear relationships and uncertainty in time series data through fuzzy logic and inference mechanisms - Capability to adapt and learn from data to optimize the fuzzy model parameters	- Complexity in designing and tuning the fuzzy inference system, including rule base construction and membership function design - Limited interpretability compared to other methods	[26]
Empirical Mode Decomposition – Support Vector Regression (EMD-SVR) method	- Effective in handling high-dimensional data and capturing nonlinear relationships - Good generalization capabilities	- Sensitivity to parameter settings and kernel selection - Limited interpretability compared to other methods	[27]
Long Short-term Memory (LSTM)	- Ability to model temporal dependencies and capture sequential patterns in time series data - Flexibility in handling various types of time series data and input features	- Suffers from vanishing/exploding gradient problems and long training times - Prone to sensitivity in parameter initialization and network architecture design	[28]
Nonlinear Autoregressive Network with Exogenous Inputs (NARX)	- Capability to capture nonlinear relationships and incorporate exogenous inputs in time series forecasting - Ability to handle time-delayed relationships	- Complexity in determining the optimal network architecture and handling long input sequences - Prone to overfitting if not properly regularized	[29]
Stack Auto Encoder (SAE)	- Effective in capturing hierarchical and abstract representations of time series data - Robustness against noise and missing data	- Increased computational complexity due to the stacked architecture - Requires careful tuning of hyperparameters such as the number of layers and hidden units	[30]
Dynamic Harmonics Regression (DHR)	- Capability to capture seasonal and harmonics components in time series data - Robustness against missing data and outliers	- Limited ability to handle complex patterns and long-term dependencies - Complexity in determining the appropriate number of harmonics components and modelling their interactions	[31]

expert information, handle uncertainties, capture nonlinear relationships, and produce findings that are easy to understand. The hybrid model can improve accuracy, resilience, flexibility, and generalisation by taking advantage of the complimentary capabilities of both methodologies, which makes it an appealing option for harmonics forecasting applications.

IV. GENERATOR MODELS

A. HYBRID WIND DFIG-PV MODEL

The hybrid wind DFIG-PV model was introduced to generate the harmonics that represented the real-world response to inputs of wind speed and solar irradiation. It was created by modifying the DFIG model from the MATLAB library and combining it with the PV model [32]. The 1.5 MW wind turbines of the hybrid wind-DFIG PV Model combine an AC/DC/AC IGBT-based PWM converter with wrapped rotor DFIG. In this concept, the wind speed signal was generated by a signal generator block. The hybrid model additionally consists of 518 parallel strings and a 1.5 MW-rated PV array. On each string, seven SunPower SPR-415E modules were connected in series. The temperature and solar irradiance for the PV model were generated by the signal generator block. As a result, the hybrid wind DFIG-PV model was constructed for a total 3 MW capacity.

The wind speed, solar irradiance, and temperature readings were taken as actual data for Halifax, Nova Scotia, Canada, between June 1 and June 24, 2015 and logged into the signal generators. The data was obtained from the Joint Research Centre (JRC) of the European Commission [33]. The generator model was simulated 19 working days using the real-world data for wind speed and solar irradiation as inputs and producing output power. Furthermore, with voltage and current waveforms from the simulated generator data the harmonics were extracted using the Fast Fourier Transform (FFT) in MATLAB. Refer to figure 2 which presents the Wind DFIG-PV model used in this work.

B. HYBRID WIND PMSG-PV MODEL

The hybrid PMSG-PV model was made by changing the PMSG model found in the MATLAB library [34] and fusing it with the PV model. The model has a multipole PMSG without a gearbox and 1.5 MW wind turbines that are coupled directly to it. Similar methodology was followed in simulating the Wind PMSG-PV generator model as Wind DFIG-PV model to obtain the output voltage and current waveforms and extract harmonics. Refer to figure 3 which presents the Wind DFIG-PV model used in this work.

C. GENERATOR MODELS SIMULATION

To record and utilize the data for simulation and forecasting, the complete data set showing the variations in wind and solar characteristics over the course of 19 working days from June 1 to June 24, 2015, was separated into datasets. The datasets used are displayed in Fig. 1:

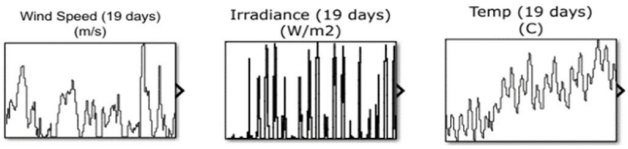

FIGURE 1. Datasets for generator models simulation.

Data was logged into the workspace and stored throughout the simulation time in a structured manner. Fig. 2 and Fig. 3 show a sample of the 3-phase voltage and current waveforms for the time period starting at 5 seconds in order to demonstrate and see the occurrence of harmonics in the waveform developed for the Wind-DFIG PV model. A zoomed view of the whole wave is shown in Fig. 2 & 3.

Harmonics can be seen in the waveforms of both voltage and current. In order to extract harmonics from the data collected from the scope, an FFT analysis was performed. The FFT samples were extracted for 432 hours (18 days), and a total of 4320 samples were recorded with 10 samples logged per hour for both current and voltage waveforms. These were grouped as training dataset to forecast the harmonics parameters for 19th day. The following harmonics parameters were extracted from the simulated signals which after statistical analysis were selected as parameters to be forecasted for both voltage and current waveforms:

1. Total Harmonics Distortion (THD)
2. Magnitude of 11th (h11) harmonics component.
3. Magnitude of 13th (h13) harmonics component.

V. FORECASTING MODELS

A. ARTIFICIAL NEURAL NETWORK (ANN)

McCulloch and Pitts published the first Artificial Neuron model in [35] that can mimic the actions of a biological neuron. An artificial neuron model functions as a sum of the products of the inputs denoted by the letter "p", the weights associated with those inputs ("w"), and the bias ("b"). To generate the output, this sum is sent through a nonlinear transfer function named "f". Weights (w) and bias are the two variables that can be altered (b). Mathematically, n is given by the following equations,

$$n = w_1 p_1 + w_2 p_2 + \cdots + w_R p_R + b \tag{1}$$

$$n = \sum_{j=1}^{R} w_j p_j + b \tag{2}$$

where $w_1, w_2 \ldots w_R$ are weights, $p_1, p_2 \ldots p_R$ are inputs, b is bias and R is number of inputs. The neuron's output is given by,

$$a = f\,(n) = f\left(\sum_{j=1}^{R} w_j p_j + b\right) \tag{3}$$

Equation (3) represents the output for a basic ANN model consisting of a single neuron and single layer. In order to improve the adaptability of ANN, it is constructed with multiple number of neurons and layers called Multi-Layer Perceptron Neural Network (MLPNN). For MLPNN with l

TABLE 2. Rationale for ANN-ANFIS based hybrid model summary.

Rationale	ANN (Artificial Neural Network)	ANFIS (Adaptive Neuro-Fuzzy Inference System)
Nonlinear Relationship Capture	ANNs excel at capturing complex nonlinear relationships between inputs and outputs. They can learn from historical data patterns and identify intricate dependencies.	ANFIS combines fuzzy logic and neural networks, enabling it to model fuzzy rules and linguistic variables. It incorporates expert knowledge into the model, capturing underlying linguistic patterns and handling uncertainties effectively.
Handling Large Volumes of Data	ANNs can efficiently handle large volumes of training data. They can process and learn from extensive datasets, which is essential in harmonics forecasting tasks where significant amounts of data are involved.	ANFIS can handle uncertain and imprecise data effectively. It can process data with varying degrees of uncertainty, providing robust predictions even in the presence of noise or incomplete information.
Adaptability and Generalization	ANNs are known for their adaptability to new patterns and variations in data. They can adjust their internal parameters and learn from evolving harmonics behaviours over time.	ANFIS can adapt its fuzzy rules and linguistic variables based on the input data. It can adjust its structure to accommodate different operating conditions and system configurations, ensuring the model's adaptability and generalization capability.
Interpretability	ANN models typically lack interpretability and are often considered as "black boxes." The complex relationships they capture can be challenging to interpret.	ANFIS provides transparency and interpretability by employing fuzzy rule-based structures. It incorporates expert knowledge and linguistic variables, allowing experts to understand and explain the decision-making process. The model's output can be easily explained using linguistic terms and fuzzy rules, making it more interpretable and explainable.
Integration of Domain Knowledge	ANN models rely primarily on data-driven learning and may not explicitly incorporate domain knowledge or expert insights.	ANFIS can incorporate domain expertise and expert knowledge into the model by defining fuzzy rules and linguistic variables. This integration helps capture the underlying dynamics and linguistic patterns specific to harmonics forecasting, enhancing the accuracy and reliability of predictions.

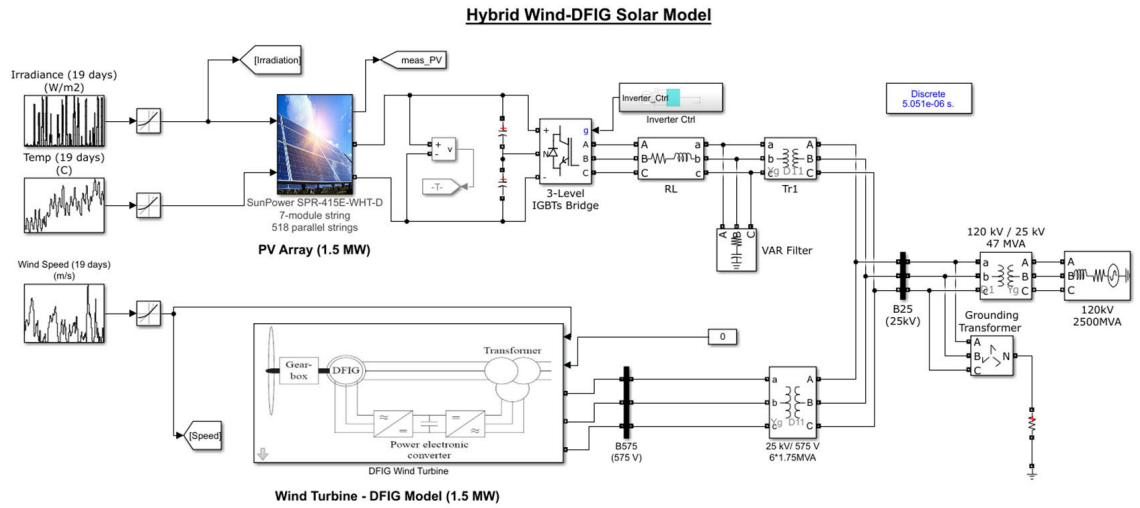

FIGURE 2. Wind-DFIG PV generator model.

number of layers and S^l number of neurons in layer l, (3) can be expressed as follows:

$$a_{lS^l} = f_l\left(n_{lS^l}\right) = f_l\left(\sum_{i=1}^{S^l}\sum_{j=1}^{S^{l-1}} w_{ij}a_{(l-1)j} + b_{lS^l}\right). \quad (4)$$

where l is the number of layers, S denotes the number of neurons, S^l denotes the number of neurons in layer l. There are three MLPNN developed in this work to be used in the hybrid forecast model. They are explained in this section.

1) 3-LAYERED CASCADED NEURAL NETWORK WITH RECURRENT LOCAL FEEDBACK (3LCRNNL)

The 3-Layered Neural Network having cascaded inputs with local feedback is portrayed in Fig. 4. This MPLNN will be termed as Three Layered Cascaded Neural Network with

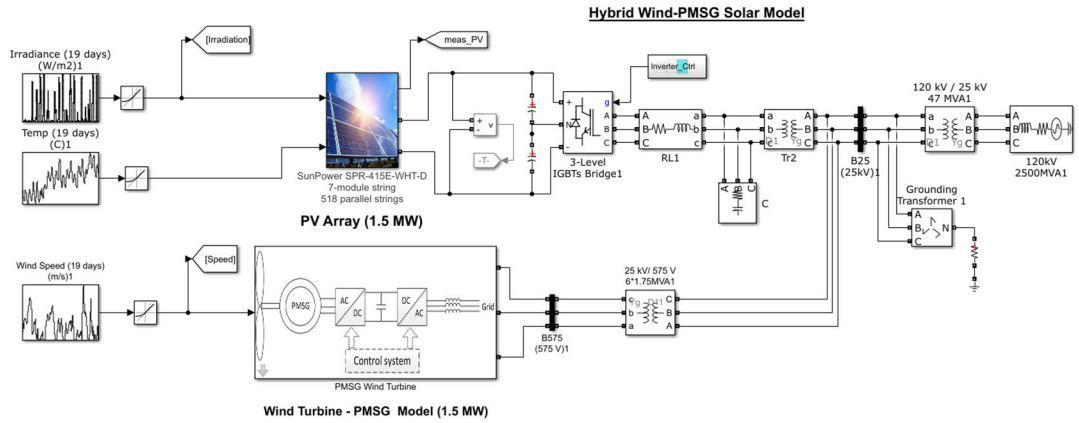

FIGURE 3. Wind-PMSG PV generator model.

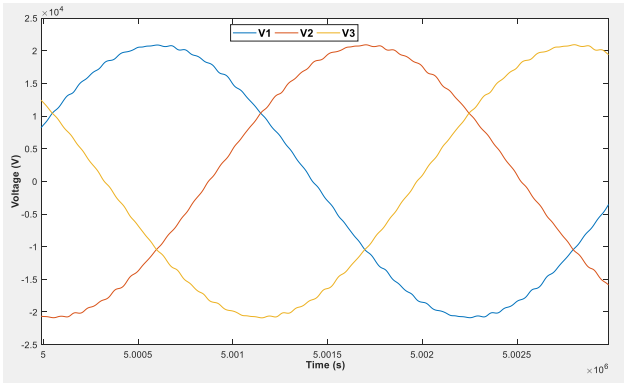

FIGURE 4. Sample voltage waveform (Wind DFIG-PV model).

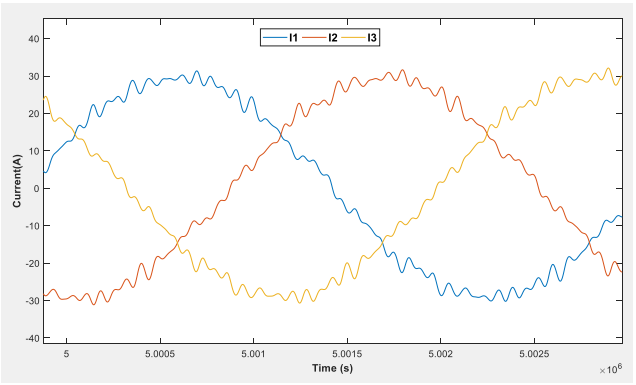

FIGURE 5. Sample current waveform (Wind DFIG-PV model).

Recurrent Local feedback (3LCNNRL). Equation (5) represents the output of the network.

$$
\begin{aligned}
a_{3S^3} &= f_3\left(n_{3S^3}\right) \\
&= f_3\Bigg(\sum_{i=1}^{S^3}\sum_{j=1}^{R} w_{ij}p_j \\
&\quad + \sum_{i=1}^{S^3}\sum_{j=1}^{S^1} w_{ij} f_1\Bigg(\sum_{i=1}^{S^1}\sum_{j=1}^{R} w_{ij}p_j \\
&\quad + \sum_{i=1}^{S^1}\sum_{j=1}^{S^2} w_{ij}a_{1j}\,(t-1) + b_{1S^1}\Bigg) \\
&\quad + \sum_{i=1}^{S^3}\sum_{j=1}^{S^2} w_{ij} f_2\Bigg(\sum_{i=1}^{S^2}\sum_{j=1}^{R} w_{ij}p_j \\
&\quad + \sum_{i=1}^{S^2}\sum_{j=1}^{S^1} w_{ij}a_{1j} \\
&\quad + \sum_{i=1}^{S^2}\sum_{j=1}^{S^2} w_{ij}a_{2j}\,(t-1) + b_{2S^2}\Bigg) \\
&\quad + \sum_{i=1}^{S^3}\sum_{j=1}^{S^3} w_{ij}a_{3j}\,(t-1) + b_{3S^3}\Bigg)
\end{aligned}
\tag{5}
$$

2) 3-LAYERED CASCADED NEURAL NETWORK WITH RECURRENT GLOBAL FEEDBACK (3LCRNNG)

The second MPLNN combines the Cascaded Neural Network with Recurrent Network with Global feedback to create Cascaded Neural Network with Recurrent Global feedback (3LCRNNG). Fig. 5 shows its construction and (6) presents its output equation.

$$
\begin{aligned}
a_{3S^3} &= f_3\left(n_{3S^3}\right) \\
&= f_3\Bigg(\sum_{i=1}^{S^3}\sum_{j=1}^{R} w_{ij}p_j \\
&\quad + \sum_{i=1}^{S^3}\sum_{j=1}^{S^1} w_{ij} f_1\Bigg(\sum_{i=1}^{S^1}\sum_{j=1}^{R} w_{ij}p_j \\
&\quad + \sum_{i=1}^{S^1}\sum_{j=1}^{S^3} w_{ij}a_{2j}\,(t-1) + b_{1S^1}\Bigg) \\
&\quad + \sum_{i=1}^{S^3}\sum_{j=1}^{S^2} w_{ij} f_2\Bigg(\sum_{i=1}^{S^2}\sum_{j=1}^{R} w_{ij}p_j \\
&\quad + \sum_{i=1}^{S^2}\sum_{j=1}^{S^1} w_{ij}a_{2j} + b_{2S^2}\Bigg) + b_{3S^3}\Bigg)
\end{aligned}
\tag{6}
$$

3) 3-LAYERED CASCADED NEURAL NETWORK WITH RECURRENT GLOBAL FEEDBACK (3LCRNNG)

As the name suggests, in order to integrate the networks to improve accuracy, in the third MPLNN, the inputs are cascaded to the next layers and each layer also receives feedback from its output as well as from the output layer. Fig. 6 below shows the architecture and (7) depicts the output of 3-Layered

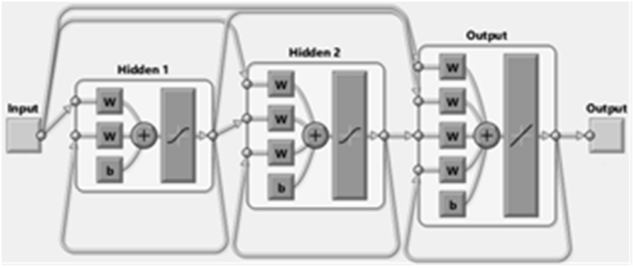

FIGURE 6. Architecture of 3LCRNNL.

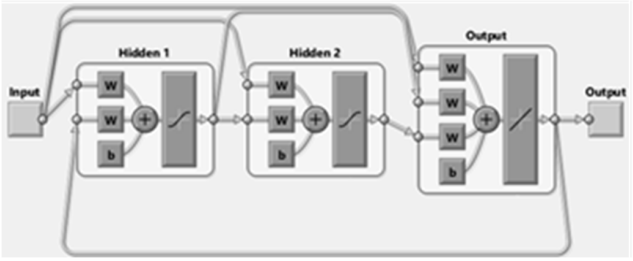

FIGURE 7. Architecture of 3LCRNNG.

Cascaded Neural Network with Recurrent Local & Global feedback (3LCRNNGL).

$$
\begin{aligned}
a_{3S^3} &= f_3\left(n_{3S^3}\right) \\
&= f_3\Bigg(\sum_{i=1}^{S^3}\sum_{j=1}^{R} w_{ij}p_j \\
&\quad + \sum_{i=1}^{S^3}\sum_{j=1}^{S^1} w_{ij} f_1\Bigg(\sum_{i=1}^{S^1}\sum_{j=1}^{R} w_{ij}p_j \\
&\quad + \sum_{i=1}^{S^1}\sum_{j=1}^{S^1} w_{ij}a_{1j}\,(t-1) \\
&\quad + \sum_{i=1}^{S^1}\sum_{j=1}^{S^3} w_{ij}a_{3j}\,(t-1) + b_{1S^1}\Bigg) \\
&\quad + \sum_{i=1}^{S^3}\sum_{j=1}^{S^2} w_{ij} f_2\Bigg(\sum_{i=1}^{S^2}\sum_{j=1}^{R} w_{ij}p_j \\
&\quad + \sum_{i=1}^{S^2}\sum_{j=1}^{S^1} w_{ij}a_{2j} + \sum_{i=1}^{S^2}\sum_{j=1}^{S^2} w_{ij}a_{2j}\,(t-1) \\
&\quad + \sum_{i=1}^{S^2}\sum_{j=1}^{S^3} w_{ij}a_{3j}\,(t-1) + b_{2S^2}\Bigg) \\
&\quad + \sum_{i=1}^{S^3}\sum_{j=1}^{S^3} w_{ij}a_{3j}\,(t-1) + b_{3S^3}\Bigg)
\end{aligned}
\tag{7}
$$

B. ADAPTIVE NEURO FUZZY INFERENCE SYSTEM (ANFIS)

In the early 1990s, the Adaptive Neuro-Fuzzy Inference System (ANFIS) was created as a result of Jang Roger's proposal to combine Adaptive Neural Networks (ANN) and Fuzzy Logic. Based on the Takagi-Sugeno Fuzzy Inference System, ANFIS combines the durability, ease of use, and convenience of implementing the rule bases of the fuzzy system with the self-learning characteristics of ANN. The ANFIS systems are particularly efficient and straightforward to build, especially in circumstances where non-linearity and data uncertainty are problems [36]. Eq. (8) demonstrates a typical fuzzy rule in a

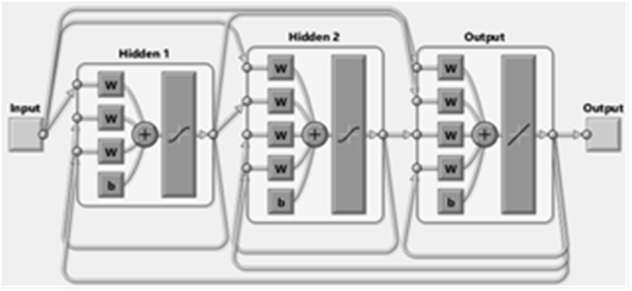

FIGURE 8. Architecture of 3LCRNNGL.

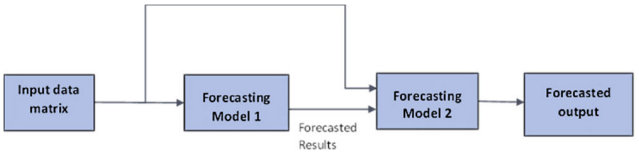

FIGURE 9. Hybrid forecasting models concept design.

Sugeno fuzzy model:

$$IF\ x\ is\ A\ and\ y\ is\ B, \quad THEN\ z = f(x, y) \tag{8}$$

where A and B are fuzzy sets, z = f (x, y) is a crisp function defining the output. The function f (x, y) is typically a polynomial which describes the output based on the input variables x and y within the fuzzy region specified by the fuzzy sets of the rule. Considering a first-order Sugeno FIS which contains two rules expressed in (9):

$$
\begin{aligned}
&Rule1\text{: } IF\ x\ is\ A1\ and\ y\ is\ B1, \\
&\qquad THEN\ f1 = p1x + q1y + r1 \\
&Rule2\text{: } IF\ x\ is\ A2\ and\ y\ is\ B2, \\
&\qquad THEN\ f2 = p2x + q2y + r2
\end{aligned}
\tag{9}
$$

The final output is a summation of all incoming signals expressed as follows:

$$f = \sum_i \bar{w}_i f_i = \frac{\sum_i \bar{w}_i f_i}{\sum_i \bar{w}_i} \tag{10}$$

C. NOVEL HYBRID FORECASTING MODELS

There are six hybrid forecasting models proposed in this work by combining the three-layered ANN models and ANFIS. The concept design of these models is depicted in Fig. 7.

The combinations for the six hybrid forecasting models are as expressed in Table 3.

The six hybrid models as expressed in Table 3 are constructed by combining ANN and ANFIS models as explained. Three types of ANN (3LCRNNL, 3LCRNNG, 3LCRNNGL) are used with hyperbolic tangent transfer function employed in hidden layers and are trained using scaled conjugate gradient algorithm. The ANFIS is used deploying the subtractive clustering technique for training network. A total of six hybrid models are proposed.

TABLE 3. Proposed hybrid models.

Proposed Hybrid Models	Forecasting Model 1	Forecasting Model 2
Model-1	3LCRNNL	ANFIS
Model-2	3LCRNNG	ANFIS
Model-3	3LCRNNGL	ANFIS
Model-4	ANFIS	3LCRNNL
Model-5	ANFIS	3LCRNNG
Model-6	ANFIS	3LCRNNGL

VI. METHODOLOGY FOR IMPLEMENTATION OF FORECASTING MODELS

A. DATA GENERATION FROM GENERATOR MODELS

To generate harmonics forecasts using the proposed hybrid models, the two generator models as discussed in section III-B were simulated for 31 days. Real-time data for wind speed and solar irradiation for Halifax was used as recorded between June 1st and 19th 2015 [57]. The generator models produce output voltage and current waveforms from which harmonics were extracted using FFT. This harmonics data was further analyzed and stored to be used as inputs for the forecasting models. The data for the 30 days (June 1st to 30th, 2015) was used for training and formed the training set, while the data for 1 day (July 1st, 2015) was used as test set.

B. SELECTION OF INPUTS

The selection of input is crucial to achieve accurate forecast. Inputs shall be carefully selected from the available data by analyzing the trends for the target signal. In order to extract harmonics, an FFT analysis was carried out on the data procured from scope. The MATLAB command line was used to extract harmonics information. The FFT window employed consist of 5 cycles which extracts the samples from voltage and current waveforms. The FFT samples were extracted for 432 hours (18 days), a total of 4320 samples were recorded with 10 samples logged per hour for both current and voltage waveforms. The following harmonics parameters were extracted from the simulated signals which after statistical analyses were selected as parameters to be forecasted for both voltage and current waveforms:

1- Total Harmonics Distortion (THD)
2- Magnitude of 11th (h11) harmonics component.
3- Magnitude of 13th (h13) harmonics component.

Additionally, the forecasting models employ various amounts of parameters for input variables (predictors) which are used as inputs to produce forecast. They are stated as follows:

1- Wind Speed
2- Solar Irradiation
3- One day before observation of predicted parameter
4- Two days before observation of predicted parameter

The selection of wind and solar irradiation was obvious as the forecasted parameters (THD, 11th, or 13th harmonics) directly depend on magnitude if wind or solar irradiation. As for the historical parameters, the one day and two days before observations, the predicted parameter has no dependencies on these inputs but rather related as at these time intervals the conditions were observed to be similar.

C. DATA PRE-PROCESSING

Data pre-processing is a step in which all data points are normalized between values of 0 and 1. This simplifies the calculations and uniformly presents all input parameters under one scale. For ANN and ANFIS implementation, it is necessary to normalize data this way for better convergence. The following formula is used to normalize data:

$$x_{norm} = \frac{x - x_{min}}{x_{max} - x_{min}} \tag{11}$$

where,

x_{norm} is the normalised data point
x is the actual data point
x_{min} is the minimum data point in the series
x_{max} is the maximum data point in the series

D. NETWORK TRAINING AND FORECASTING

1) APPLICATION OF ARTIFICIAL NEURAL NETWORKS

The ANN models used in this work aim to predict the next step harmonics. The ANN uses previously observed harmonics patterns of simulated data for training and learning in order to provide forecasts. Furthermore, for the ANN to work well, there must be a strong correlation between the inputs and outputs. Additionally, in order to improve performance, the hidden layer and output layer weights must be carefully adjusted throughout the training phase [31]. Hence, determining the architecture specifically, the ideal number of hidden layers, the number of neurons in each layer, and the role of each layer's activation becomes essential for better performance [25]. In order to improve weight adjustment, the hyperbolic tangent transfer function was used for the hidden layers. By default, MATLAB uses sigmoid transfer function. For a complex and non-linear dataset as employed in this research, the selection of hyperbolic transfer function is more beneficial as compared to the sigmoid function. Figure 8 superimposes the sigmoid function over the hyperbolic tangent function [37].

Figure 8 establishes two features that differentiate hyperbolic tangent function with sigmoid function.

1- The sigmoid function has a substantially smaller slope than the hyperbolic tangent function;
2- The sigmoid function always responds positively, but the hyperbolic tangent function responds negatively for negative input values and positively for positive input values.

The larger slope of the hyperbolic tangent function indicates that it responds more strongly to even a modest change in the input variable. As a result, it can provide a considerably more nonlinear response and can better distinguish between subtle variations in the input variable. For network nodes, it is also crucial that the sign of the response coincides with the

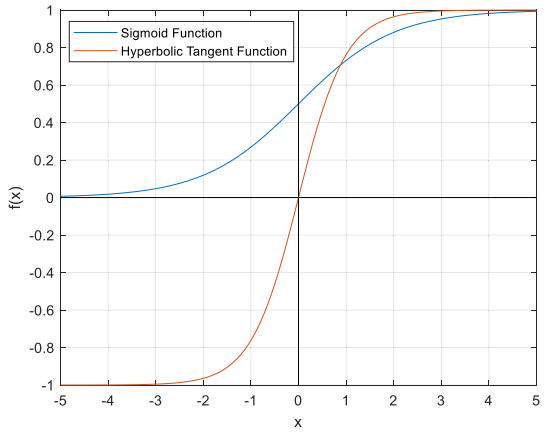

FIGURE 10. Superimposed hyperbolic function over sigmoid function.

sign of the input in the hyperbolic tangent transfer function. With normalizing and standardizing the data to the zero mean gives a node's output value some meaning. A node's average state is represented by 0, the lowest response level is represented by -1, and the highest response level is represented by +1. With this structure, the inputs to the nodes of the first hidden layer are similarly zero when the input variables are nominally zero. Consequently, when applying a hyperbolic tangent transfer function, the outputs of such nodes are also zero. The output layer's inputs and outputs are all zero, as are those of the other hidden layers. In other words, the network already accurately predicts the nominal situation before any training even begins, thus it essentially only must be trained for deviation from the nominal case. In contrast, a 0 input to a sigmoid transfer function results in an output response of 0.5, indicating that the network must additionally modify its initial weights in order to train the nominal case, reducing the effectiveness of training. The 3LCNNRL, 3LCNNRG, and 3LCNNRGL ANN models and architecture used in this work employ the hyperbolic tangent transfer function in all their hidden layers.

Additionally, the ANN models employ various amounts of parameters for input variables (predictors), including Solar Irradiation, Wind Speed, and historical values for the forecasted parameter (i.e., one hour, one day and two days before). Moreover, the ANN models employ scaled conjugate gradient as an optimizer for the reduction of the error function (training). This optimal harmonic prediction optimizer was identified by trial and error. Based on conjugate directions, Moller [38] created the scaled conjugate gradient (SCG) algorithm. Unlike other conjugate gradient algorithms, which need a line search at each iteration, this technique does not do a line search at each iteration; SCG was created to do away with the tiresome line search. A network training function called ''trainscg'' in MATLAB changes bias and weight variables using the scaled conjugate gradient approach.

If the weights, net input, and transfer functions contain derivatives, it can train any network. The quadratic approximation of the error function is used to determine the step size in the SCG algorithm, which further increases its robustness and independence from user-defined parameters [39].

2) APPLICATION OF ADAPTIVE NEURO FUZZY INFERENCE SYSTEM (ANFIS)

The adaptive neuro fuzzy inference system (ANFIS) is a hybrid system that combines the advantages of both ANN and the fuzzy system [26], [31]. As a result, the ANFIS ought to be more accurate in making predictions than the ANN. In order to model data uncertainty, ANFIS essentially combines the learning capabilities of NNs with those of an FIS. It is simple to train an ANFIS model without the need for detailed subject-matter expertise. ANFIS has the benefit of utilizing both verbal and numerical information. Thus, the flexibility, nonlinearity, and quick learning of ANFIS are its benefits. However, the system becomes exceedingly challenging to execute practically when the number of inputs to the standard ANFIS system's fuzzy system rises. Additionally, as more inputs and membership functions are selected for each input, the more training time is needed for the standard ANFIS system. Additionally, as the number of membership functions per input increases, so do the fuzzy rules. Using the ANFIS method for prediction, which is based on clustering, makes it simple to overcome the challenges listed above.

Subtractive clustering is a quick procedure for figuring out how many clusters there are and where their centres are for making predictions. Moreover, it is also very useful when data characteristics are uncertain to be clustered. The subtractive clustering method is an extension of the mountain clustering method proposed in [40]. This method evaluates each data point as a prospective cluster centre candidate and then determines each data point's potential by calculating the density of the data points around it. When it is unclear how many data distribution centres will be needed, this strategy is used. This is the case in this research due to which subtractive clustering is used. The approach is iterative, and it assumes that any point could serve as the centre of a cluster depending on where it is in relation to other data points. It involves selecting the point with the best likelihood of being the cluster centre, then deleting every other point inside the first cluster centre's radius (the radius is defined by the neighbourhoods of the centre). Additionally, to find the next cluster centre, recalculate the potential of the other spots. Finally, keep doing this until all the data is contained within a cluster centre's radius [41]. The following steps sums up the algorithm:

1. Based on the density of nearby data points, determine the likelihood that each data point would define a cluster centre. Measure density index D_i corresponding to data x_i as expressed in (12).

$$D_i = \sum_{j=1}^{n} \exp\left(-\frac{\|x_i - x_j\|^2}{\left(r_a/2\right)^2}\right) \tag{12}$$

where,

r_a = positive number that represents the radius where all the data within it are considered neighborhoods;

2. Pick the data point that has the best chance of becoming the first cluster centre. Hence, the data point with the highest density measure is selected as the first centre cluster denoted x_{c1} and its density is D_{c1}.

3. Eliminate all data points close to the first cluster centre. With the use of cluster influence range, the area is identified.

4- Recalculate the density measurements for each data point xi and select the final point with the greatest potential to serve as the cluster centre expressed in (13).

$$D_i' = D_i - D_{cl} \exp\left(-\frac{\|x_i - x_{c1}\|^2}{\left(r_b/2\right)^2}\right) \tag{13}$$

where,

$r_b = \mathrm{K} r_a$ (K is a positive number, usually K = 1.5 [41]).

All the points near to the first cluster centre x_{c1} will have low-density degree and thus they will not be considered as the next cluster centres. The next cluster centre x_{c2} is nominated after the density measure for each data point is recalculated.

5- Keep going back and forth between steps 3 and 4 until a cluster centre can affect all the data.

For optimization, the following parameters were changes to improve the performance. Specify the following clustering options:

- Squash factor - Only find clusters that are far from each other.
- Accept ratio - Only accept data points with a strong potential for being cluster centres.
- Reject ratio - Reject data points if they do not have a strong potential for being cluster centres.

In this work, the ANFIS is utilized using subtractive clustering which is optimized by trial and error. The input parameters (predictors) used in ANFIS are the same as those used for ANN.

E. MODELS 1-3: 3LCNNRL-ANFIS, 3LCNNRG-ANFIS, 3LCNNRGL-ANFIS

The 3 layered neural networks with cascaded inputs and recurrent feedbacks as utilized in models 1-3 have 8 nodes in the first hidden layer and 16 nodes in the second hidden layer. The number of layers selected are optimized to give the best performance. The optimization was done by trial-and-error method by using different combinations of hidden and output layers in stage one with the ANN, which are trained using the Scaled-Conjugate Gradient backpropagation due to its fast convergence with a large amount of data. Furthermore, hyperbolic tangent transfer function is used in the hidden layers to adjust weights to make the model synchronized with the input trends. To further improve adaptability, ANFIS is used in the second stage of the hybrid models with subtractive clustering to make the comprehensive hybrid structure robust in order to generate accurate responses for forecasting.

Once the ANN in the first stage of the models is trained using the training dataset, the results are forecasted. All four inputs of the training dataset are then fed to the ANFIS model in the second stage in addition of the fifth input, which are the forecasted results from stage one. This additional input from forecasting results from neural networks is expected to refine the final output.

F. MODELS 4-6: ANFIS-3LCNNRL, ANFIS-3LCNNRG, ANFIS-3LCNNRGL

For proposed hybrid models 4-6, the ANFIS is used to forecast results for the 19th day in the first stage using training dataset. Further, the results from ANFIS are fed into the neural networks along with the four inputs. Hence, the structure of ANN utilized in the second stage has 10 nodes in the first hidden layer and 20 nodes in the second. Scaled-Conjugate Gradient backpropagation method is used for training the ANNs and hyperbolic tangent used as transfer function to adjust weights in the stage 2 for proposed hybrid models 4-6.

G. EVALUATION OF FORECASTING MODELS

The performance of forecasting models is evaluated using the percentages of Mean Absolute Error (MAE%) and Root Mean Squared Error (RMSE%) indices. When a model's mean absolute error (MAE) and root mean square error (RMSE) are both smaller, it performs better. With time step N, target sequence denoted by t_i while forecast sequence by f_i, $i$denotes the datapoint, (11) and (12) presents the formulas to calculate the RMSE% and MAE%:

$$RMSE(\%) = \sqrt{\frac{1}{N}\sum_{i=1}^{N}(t_i - f_i)^2} \times 100 \tag{14}$$

$$MAE(\%) = \frac{1}{N}\sum_{i=1}^{N}|t_i - f_i| \times 100 \tag{15}$$

VII. RESULTS

A. HARMONICS FORECASTING – WIND DFIG-PV MODEL

1) VOLTAGE HARMONICS

The actual versus forecast curves for six proposed hybrid models for wind DFIG-PV are presented in Fig. 8, 9 and 10 along with the forecasting result curves of all individual models (i.e., 3LCRNNL, 3LCRNNG, 3LCRNNGL and ANFIS). There are a total of three variables that have been forecasted. The major one is the Voltage Total Harmonics Distortion (THDV) followed by the individual dominant harmonics 11th (h11) and 13th (h13). To further analyze the error profile and accuracy of these models, refer to Table 2 which presents the metrics calculated (RMSE and MAE). From Table 2 it can be observed that model-3 produces the best results with the lowest RMSE (8.420%) and MAE (4.601%). Which means overall datapoints variation of ±8.420% for model-3 which has proven to be the most accurate as compared to the other models. Furthermore, the results of individual models are also presented. ANFIS is the best performing individual model with 8.844% RMSE and 5.55% MAE. By using hybrid model, it is evident that the overall forecasting error produced by each individual model has shown improvement.

Results shown in Table 4, further suggest for 11th harmonics (h11), model 4 and for 13th harmonics (h13), model-2 perform best with the lowest RMSE%. Specifically, for h11

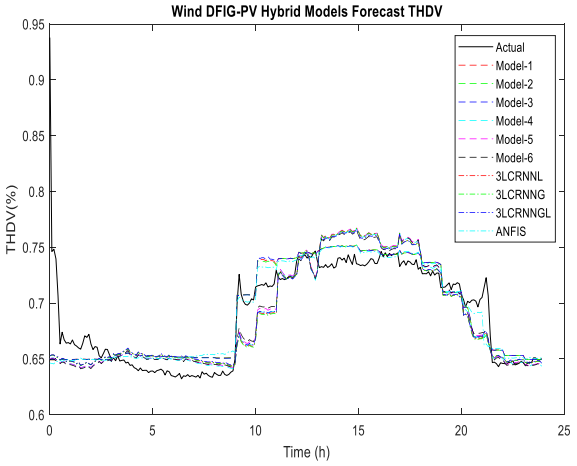

FIGURE 11. THDV – actual vs forecast curves wind DFIG-PV model.

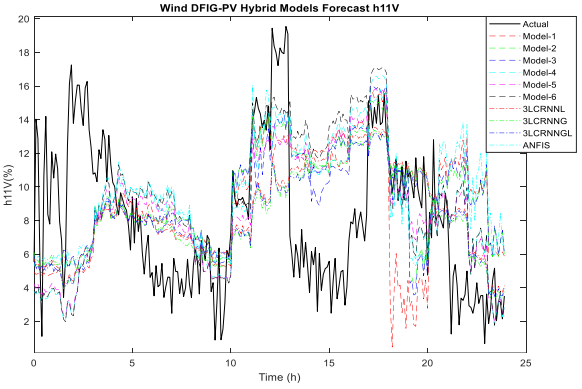

FIGURE 12. Voltage 11th harmonics – actual vs forecast curves wind DFIG_PV model.

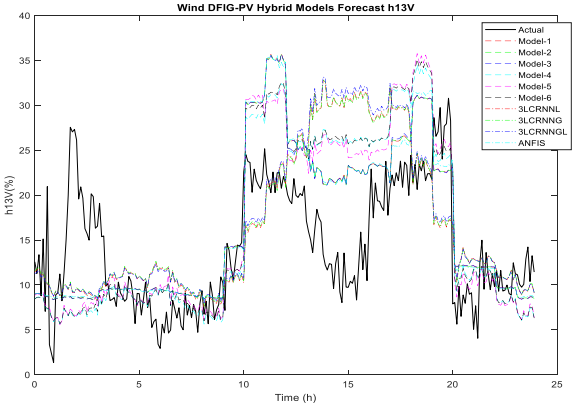

FIGURE 13. Voltage 13th harmonics – actual vs forecast curves wind DFIG_PV model.

the RMSE% for model 4 is 11.262% which is the lowest, but if MAE% is observed, the individual model 3LCNNRGL produces the lowest MAE% of 8.975%. Whereas, for h13, model-2 performs best in terms of RMSE% as well as MAE% having values of 10.941% and 8.537% correspondingly. It can be observed that for the case of individual harmonics

TABLE 4. THD, 11th and 13th voltage harmonics forecast results for wind DFIG-PV model.

Forecasting Models	THDV		h11		h13	
	RMSE (%)	MAE (%)	RMSE (%)	MAE (%)	RMSE (%)	MAE (%)
Model-1	8.54%	4.74%	11.92%	9.73%	11.05%	8.72%
Model-2	8.42%	4.61%	12.39%	10.15%	10.94%	8.53%
Model-3	8.42%	4.60%	11.73%	9.57%	10.94%	8.53%
Model-4	8.80%	5.48%	11.26%	9.32%	12.20%	9.41%
Model-5	8.75%	5.45%	11.51%	9.55%	12.16%	9.35%
Model-6	8.83%	5.57%	11.38%	9.40%	12.30%	9.40%
3LCRNNL	9.29%	5.68%	11.39%	9.03%	14.35%	10.43%
3LCRNNG	9.09%	5.49%	11.58%	9.14%	13.77%	10.10%
3LCRNNGL	9.13%	5.54%	11.33%	8.97%	13.77%	10.09%
ANFIS	8.84%	5.55%	11.39%	9.43%	12.39%	9.52%

forecasting, the improvement of hybrid model over individual ones is not significant. Though there is a small improvement while using models in the hybrid framework, ANFIS again performed better than the rest of the individual models. The percentages RMSE for THDV as compared to the dominant harmonics forecast are lower. Model-4 (ANFIS-3LCNNRL) and model-2 (3LCNNRG-ANFIS) achieved healthier results for h11 and h13 harmonics respectively.

2) CURRENT HARMONICS

This section presents the actual versus forecasted curves for the individual as well as the six proposed hybrid models used to predict the THDI, h11 and h13 harmonics. Fig. 11, 12 and 13 presents the forecast curves for THDI, h11 and h13 forecast which is followed by Table 5 summarizing the performance of each model for THDI, 11th and 13th current harmonics.

Model-6 fits the actual curve better than the other models for THDI forecasts, as seen in the Figures and Tables above with the lowest RMSE (0.336%) as well as MAE (0.242%). Model 1 produces the least MAE with 0.229%. Model-5 has the lowest RMSE & MAE for h11, while model-3 has the best result statistics for h13. The RMSE percent for THDI is 0.341% for model-1, indicating that the predicted points are extremely close to the actual. In the case of h11, the results show that model-4 outperforms the others in terms of all performance metrics. Model-3, on the other hand, has the lowest percent RMSE of 11.516% and MAE of 9.012, making it the best predictor model for h13.

It may be concluded that all six proposed models predicted current total harmonics distortion correctly and produced improved results as compared to the individual models, with RMSE% and MAE% relatively low. For THDI, very low RMSE and MAE of 0.341% and 0.229% corresponds to very low forecast dispersion around the actual curve. Models 5 and 3, which use the ANFIS-3LCNNRG and 3LCNNRGL-ANFIS structures respectively, outperformed all other models

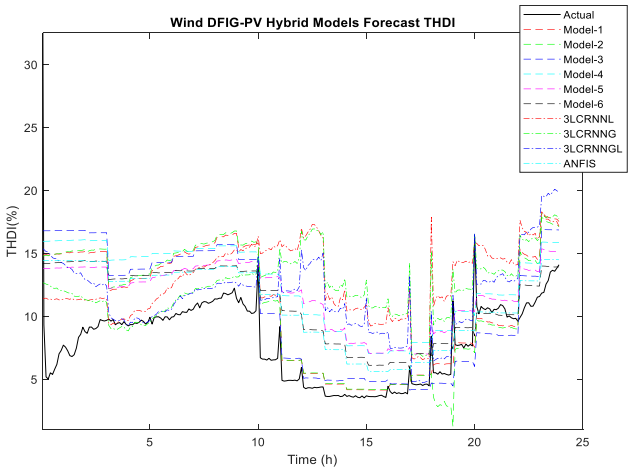

FIGURE 14. THDI – actual vs forecast curves Wind DFIG-PV model.

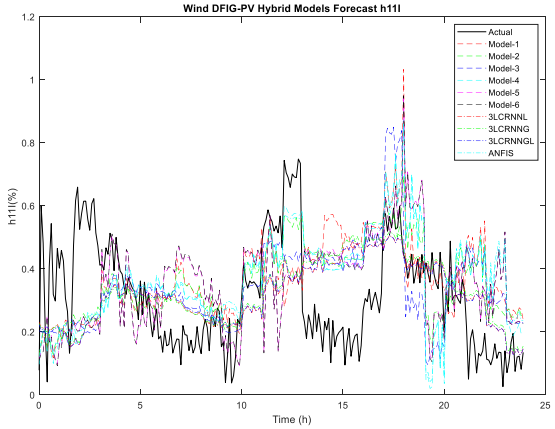

FIGURE 15. Current 11th harmonics – actual vs forecast curves Wind DFIG_PV model.

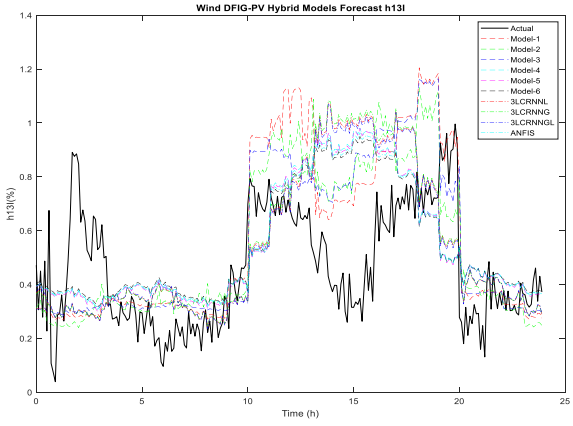

FIGURE 16. Current 13th harmonics – actual vs forecast curves wind DFIG_PV model.

for the individual harmonics h1 and h13. The improvement of performance for hybrid models over individual ones are not noteworthy for h11 and h13 which suggests that it requires a different approach to forecast these parameters accurately.

TABLE 5. THD, 11th and 13th current harmonics forecast error for wind DFIG-PV model.

Forecasting Models	THDI		h11		h13	
	RMSE (%)	MAE (%)	RMSE (%)	MAE (%)	RMSE (%)	MAE (%)
Model-1	0.34%	0.22%	17.51%	12.92%	11.83%	9.25%
Model-2	0.35%	0.23%	11.68%	9.68%	11.64%	9.23%
Model-3	0.35%	0.24%	12.52%	10.54%	11.51%	9.01%
Model-4	0.40%	0.33%	11.61%	9.65%	12.29%	9.45%
Model-5	0.36%	0.28%	11.41%	9.46%	12.25%	9.38%
Model-6	0.34%	0.24%	11.47%	9.52%	11.86%	9.19%
3LCRNNL	0.44%	0.35%	11.43%	9.12%	13.16%	9.61%
3LCRNNG	0.47%	0.37%	11.62%	9.22%	13.42%	9.77%
3LCRNNGL	0.37%	0.26%	11.37%	9.04%	13.04%	9.55%
ANFIS	0.66%	0.34%	11.51%	9.56%	12.04%	9.26%

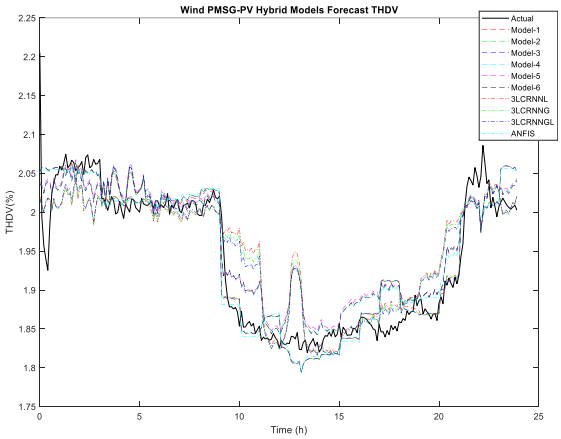

FIGURE 17. THDV – actual vs forecast curves wind PMSG-PV model.

B. HARMONICS FORECASTING – WIND PMSG-PV MODEL

1) VOLTAGE HARMONICS

The actual versus predicted curves for all six proposed hybrid models and the individual forecasting models for wind PMSG-PV model are shown in Fig. 14, 15 and 16 for Voltage harmonics parameters. The forecast curves are followed by Table 6 summarizing the error profile of each forecast made for each variable.

From results presented in Table 5, it can be observed that as compared to DFIG, the forecast for all 3 cases to predict the voltage harmonics have shown much better results. By observing Table 5, it can be concurred that the overall performance of all models has shown accurate predictions with percent RMSE and MAE for all hybrid models below 5%, which suggests that each model predicted quite accurately. To single out the best performing model, model-1 employing 3LCNNRL-ANFIS has proved to be the best in terms of all error performance matrices, with RMSE of 3.963% and MAE of 2.619%. Additionally, a substantial improvement from using hybrid models over individual ones for forecasting

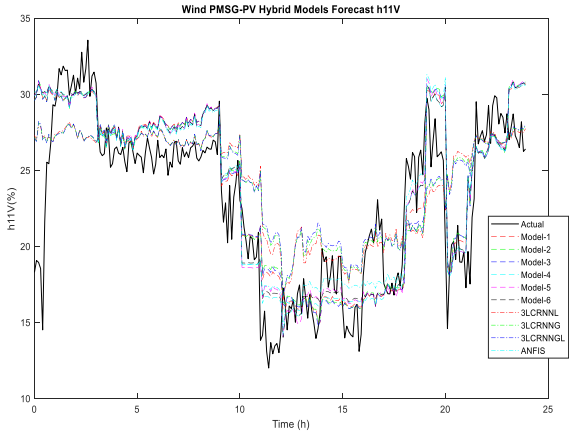

FIGURE 18. Voltage 11th harmonics – actual vs forecast curves wind PMSG_PV model.

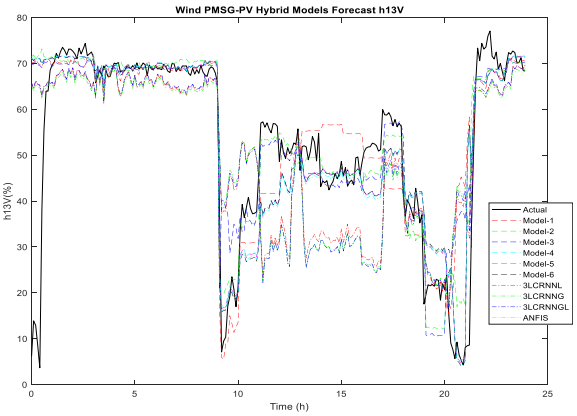

FIGURE 19. Voltage 13th harmonics – actual vs forecast curves wind PMSG_PV model.

TABLE 6. THD, 11th and 13th voltage harmonics forecast error for wind PMSG-PV model

Forecasting Models	THDV		H11		H13	
	RMSE (%)	MAE (%)	RMSE (%)	MAE (%)	RMSE (%)	MAE (%)
Model-1	3.93%	2.61%	9.61%	7.05%	16.26%	8.72%
Model-2	3.95%	2.65%	9.93%	7.29%	13.67%	6.58%
Model-3	3.96%	2.65%	9.83%	7.24%	15.23%	7.57%
Model-4	4.61%	3.56%	9.39%	6.86%	14.62%	7.58%
Model-5	4.74%	3.72%	9.41%	6.93%	14.61%	7.56%
Model-6	4.66%	3.61%	9.35%	6.85%	14.68%	7.66%
3LCRNNL	5.28%	3.90%	11.41%	8.88%	20.04%	14.09%
3LCRNNG	5.58%	4.10%	11.35%	8.80%	20.20%	14.49%
3LCRNNGL	5.91%	4.29%	11.38%	8.83%	19.24%	13.47%
ANFIS	3.96%	2.80%	10.30%	6.85%	14.70%	7.68%

is determined by the results presented. For h11, model-6 (ANFIS-3LCNNRGL) performs better than all others. Overall results have shown low RMSE% and MAE% with 9.35% and 6.851% being the lowest respectively for model 6. For

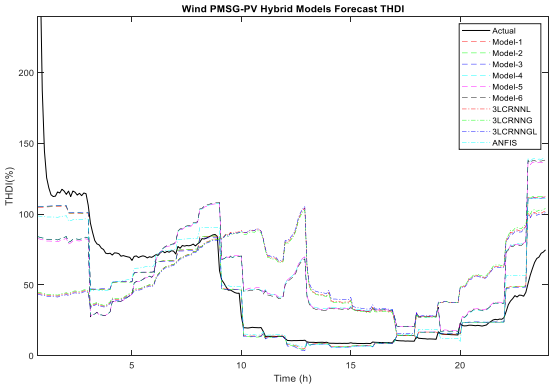

FIGURE 20. THDI – actual vs forecast curves Wind PMSG-PV model.

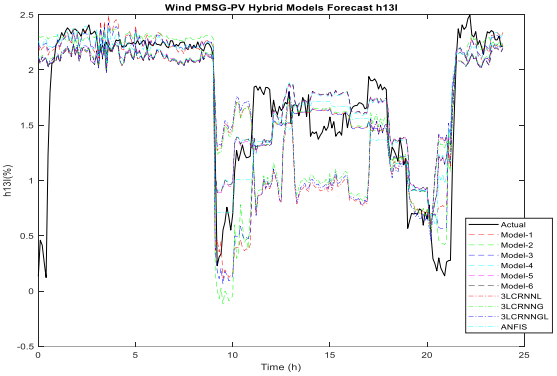

FIGURE 21. Current 11th harmonics – actual vs forecast curves wind PMSG_PV model.

h13 forecast, model-2 (3LCNNRG-ANFIS) has been the clear standout as compared to other models with 13.671% RMSE and 6.582% MAE. Further, it can be observed that ANFIS has outperformed all other neural network based individual forecasting models for all the cases.

2) CURRENT HARMONICS

The actual vs anticipated curves for the proposed forecasting models used to predict the current harmonics for wind PMSG-PV model is presented in Fig. 17, 18 & 19. The performance stats for forecasts for THDI, h11 and h13 for current waveform are presented in Tables 7.

As seen in Fig. 17, 18 & 19 and Table 7, Model-3 (CNNRGL-ANFIS) fits the real curve better than the other models for THDI, with the lowest RMSE (6.901%) and MSE (0.941%). The results reveal that model-6 surpasses the others in terms of both performance measures for forecasting h11 with models 4 & 5 also generating good results with RMSE and MAE of around 7.6% and 5.5% with the lowest reaching to 7.616% and 5.569% for model 6 (ANFIS-3LCNNRGL). Among individual models, ANFIS produces results as good as models 4, 5 and 6 with RMSE 7.652% and MAE 5.568%. The hybrid models seem to offer similar results to ANFIS. Furthermore, for h13, model-5 (ANFIS-3LCNNRG) has the lowest percent RMSE (14.97%) and MAE (9.458%).

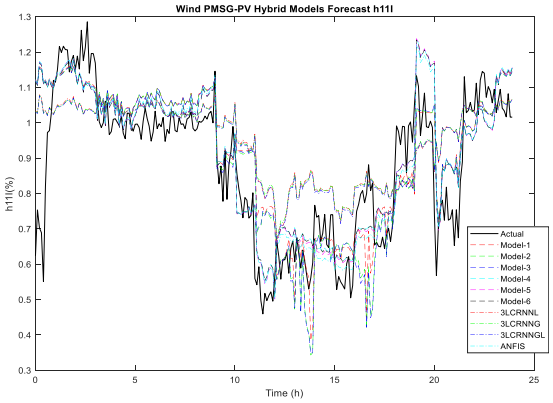

FIGURE 22. Current 13th harmonics – actual vs forecast curves wind PMSG_PV model.

TABLE 7. THD, 11th and 13th current harmonics forecast error for wind DFIG-PV model.

Forecasting Models	THDI		H11		H13	
	RMSE (%)	MAE (%)	RMSE (%)	MAE (%)	RMSE (%)	MAE (%)
Model-1	3.93%	2.61%	9.61%	7.05%	16.26%	8.72%
Model-2	3.95%	2.65%	9.93%	7.29%	13.67%	6.58%
Model-3	3.96%	2.65%	9.83%	7.24%	15.23%	7.57%
Model-4	4.61%	3.56%	9.39%	6.86%	14.62%	7.58%
Model-5	4.74%	3.72%	9.41%	6.93%	14.61%	7.56%
Model-6	4.66%	3.61%	9.35%	6.85%	14.68%	7.66%
3LCRNNL	5.28%	3.90%	11.41%	8.88%	20.04%	14.09%
3LCRNNG	5.58%	4.10%	11.35%	8.80%	20.20%	14.49%
3LCRNNGL	5.91%	4.29%	11.38%	8.83%	19.24%	13.47%
ANFIS	3.96%	2.80%	10.30%	6.85%	14.70%	7.68%

VIII. ANALYSIS OF RESULTS

This section presents a comparison between the forecasting outcomes generated by the hybrid models suggested in this work and the forecasting techniques used by the work done in the literature. References [23], [24], and [25] for different types of ANN, [26] for ANFIS, and [27] for LSTM (Long Short-Term Memory) network approaches are used as examples to compare the proposed work with as a way of validation.

Three Neural Networks are chosen from among the methods used in [23], [24], and [25] to accomplish the forecasting for this work. Cascaded Recurrent Neural Network with Local Feedback (CNNRL), Cascaded Recurrent Neural Network with Global Feedback (CNNRG), and Cascaded Recurrent Neural Network with Local and Global Feedback (CNNRGL) are these networks. In addition, [26] uses ANFIS and [27] adopted the LSTM approach for forecasting. These 5 approaches are used to draw a comparative analysis in which the same data used in this work is utilized for all different forecasting methods stated. Percent Root Mean Squared Error (RMSE%) and percent Mean Absolute Error (MAE%) are the indices used to compare the results.

A. UTILIZATION OF ARTIFICIAL NEURAL NETWORK (ANN)

References [23], [24], and [25] apply ANN models to forecast harmonics. Three Neural Networks are chosen from among the methods utilized in these papers to forecast and compare. The data used to forecast is the same 18 days data which is employed in this work generated by the simulation of two hybrid models. The four inputs used are wind speed, solar irradiation, day before and two days before observations of forecasted parameters. Each version of ANN has a first hidden layer with eight nodes, and a second layer with sixteen nodes.

B. UTILIZATION OF ADAPTIVE NEURO FUZZY INFERENCE SYSTEM(ANFIS)

Reference [26] employ ANFIS architecture to forecast voltage and current THD. In order to draw comparison ANFIS is utilized with the data used in this work with four inputs as stated in section VI-A. Subtractive clustering is used to optimize the training process. Along with THD, h11 and h13 are also forecasted. The results produced from ANFIS system are presented in section VI-D to draw comparison with models proposed in this work.

C. UTILIZATION OF LONG-SHORT TERM MEMORY NETWORK(LSTM)

Reference [27] utilize the deep learning LSTM method for forecasting harmonics. The same simulated data and four inputs are used to generate forecast for THD, h11 and h13 for voltage and current for the two generator models. The LSTM utilized consists of four sequence input layers, two hundred LSTM layers, one fully connected layer, a regression layer, and an output layer. Since there are four inputs, the size of the input layer is set to four. The two hundred hidden layers of the LSTM layer are utilized to execute additive interactions and learn long-term relationships between sequence and time series data. The forecast is being generated in MATLAB and presented in sections VI-D for comparison with the hybrid models used in this work.

D. RESULTS VALIDATION – WIND DFIG-PV MODEL

1) VOLTAGE HARMONICS

Table 8 provides a comparative analysis of the six proposed forecasting models for wind DFIG-PV generator model for Voltage harmonics.

The proposed hybrid models utilized in this work and the forecasting techniques employed by other researchers are shown in Table 8 together with their respective findings' RMSE% and MAE%. The list of references where each of these techniques was employed by the authors are mentioned at the bottom of the table. Therefore, by contrasting the results with CNNRL, CNNRG, CNNRGL, ANFIS and LSTM, the

TABLE 8. Result comparison for wind DFIG-PV model – voltage harmonics.

Forecasting Models	THDV		h11		h13	
	RMSE (%)	MAE (%)	RMSE (%)	MAE (%)	RMSE (%)	MAE (%)
Model-1[1]	8.54%	4.74%	11.92%	9.73%	11.05%	8.72%
Model-2[1]	8.52%	4.71%	12.39%	10.15%	10.94%	8.53%
Model-3[1]	8.42%	4.60%	11.73%	9.57%	*10.94%*	*8.53%*
Model-4[1]	8.80%	5.48%	11.26%	9.32%	12.20%	9.41%
Model-5[1]	8.75%	5.45%	11.51%	9.55%	12.16%	9.35%
Model-6[1]	*8.53%*	*5.37%*	*11.38%*	*9.40%*	12.30%	9.40%
CRNNL[2]	9.18%	5.58%	11.58%	9.18%	13.45%	9.85%
CRNNG[2]	9.21%	5.59%	11.42%	9.01%	13.40%	9.82%
CRNNGL[2]	9.06%	5.47%	11.40%	9.04%	13.80%	10.05%
ANFIS[3]	8.46%	4.69%	12.29%	10.23%	11.89%	9.46%
LSTM[4]	8.792%	5.10%	11.86%	9.15%	15.07%	10.86%

[1] Proposed Models
[2] Publication [23], [24] & [25]
[3] Publication [26]
[4] Publication [27]

TABLE 9. Result comparison for wind DFIG-PV model – current harmonics.

Forecasting Models	THDV		h11		h13	
	RMSE (%)	MAE (%)	RMSE (%)	MAE (%)	RMSE (%)	MAE (%)
Model-1[1]	0.34%	0.23%	17.51%	12.92%	11.83%	9.25%
Model-2[1]	0.35%	0.24%	11.68%	9.68%	11.64%	9.233%
Model-3[1]	0.36%	0.25%	12.52%	10.54%	11.51%	9.01%
Model-4[1]	0.40%	0.33%	11.61%	9.65%	12.29%	9.45%
Model-5[1]	0.36%	0.28%	11.41%	9.46%	12.25%	9.38%
Model-6[1]	*0.34%*	*0.24%*	*11.47%*	*9.52%*	*11.56%*	*9.19%*
CRNNL[2]	0.44%	0.34%	11.43%	9.06%	13.42%	9.79%
CRNNG[2]	0.47%	0.37%	11.67%	9.26%	13.06%	9.57%
CRNNGL[2]	0.37%	0.26%	11.43%	9.05%	13.26%	9.68%
ANFIS[3]	0.66%	0.34%	13.01%	11.09%	11.64%	9.79%
LSTM[4]	0.40%	0.28%	13.18%	10.13%	13.04%	10.22%

[1] Proposed Models
[2] Publication [23], [24] & [25]
[3] Publication [26]
[4] Publication [27]

benefit of utilizing a hybrid technique can be seen. The most accurate model for forecasting THDV is Model 3, which has RMSE% of 8.42% and MAE% of 4.601%. Additionally, Models 2 and 3 are the only techniques that delivered outcomes better than ANFIS which is the best performing model among individual models with RMSE of 8.46% and MAE of 4.69%. Furthermore, when RMSE is considered, Model 4 has the lowest value of 11.262% for the prediction of the eleventh harmonics. Model 2 achieves the best and most accurate results for the thirteenth voltage harmonics in terms of both metrics (RMSE 10.941% and MAE 8.537%). Finally, it is also noteworthy that the second-best results have been produced by model 6 for THDV and 11th voltage harmonics and model 3 for 13th voltage harmonics.

2) CURRENT HARMONICS

Table 9 presents a comparative analysis of the six proposed forecasting models for Wind DFIG-PV generator model for current harmonics for the purpose of comparing results.

Table 9 shows that Model 6 surpasses all other models in terms of performance indices for the forecast of the current THD having the lowest RMSE (0.336%) and MAE (0.229%). For the eleventh harmonics Model 5 produces the best results with 11.411% RMSE and 9.465% MAE. In addition, Model 3 has the lowest RMSE for the thirteenth current harmonics at 11.516% RMSE and 9.012% MAE. Furthermore, model 6 have yielded the second-best performance all the cases for the current harmonics (THDI, h11 and h13) for wind-DFIG PV generator model.

3) RESULT SUMMARY – WIND DFIG-PV MODEL

Voltage model-3, which employed a combination of 3 layered cascaded recurrent neural network with local and global feedback, recorded the best performance for THDV, whereas for h11 and h13 model-4 and model-2 produced the best results. For current harmonics, model-1 proved to be the most accurate for THDI, while model-5 and model-3 provided the best results for h11 and h13 respectively. Table 10 manifests the best forecasting models and the percentage improvements they offer with respect to RMSE over forecasting models used by other authors for the DFIG-PV generator model. It can be observed that the best performing hybrid models offer improvements over all the individual models. For instance, the model-3 for voltage THD has RMSE 8.42% while LSTM with RMSE 8.792% is greater than that produced by model-3. This refers to a 4.2% improvement in prediction results produced by hybrid model-3 over LSTM forecast. Similarly, for other forecasting models the hybrid model-3 produces an improvement of 0.5% over ANFIS, 8.3% over CNNRL, 8.6% over CNNRG and 7.1% over results produced by CNNRGL respectively.

E. RESULTS VALIDATION – WIND PMSG-PV MODEL

1) VOLTAGE HARMONICS

Table 11 provides a comparative analysis of the six proposed forecasting models for wind PMSG-PV generator model for Voltage harmonics. The most accurate results for THDV, h11, and h13 harmonics were produced by model 1 (RMSE 3.93%, MAE 2.61%), model 6 (RMSE 9.35%, MAE 6.85%), and model 2 (RMSE 13.67%, MAE 6.58%), accordingly for

TABLE 10. Best forecast for DFIG-PV model.

	Best Models	RMSE (%)	RMSE (% Improvement)				
			LSTM	ANFIS	CRNNL	CRNNG	CRNNGL
Voltage	M3-THDV	8.420%	8.792% (4.2%)	8.460% (0.5%)	9.186% (8.3%)	9.210% (8.6%)	9.064% (7.1%)
	M4-h11V	11.262%	11.867% (5.1%)	12.292% (8.4%)	11.585% (2.8%)	11.424% (1.4%)	11.890% (5.3%)
	M2-h13V	10.941%	15.076% (27.4%)	11.01% (0.6%)	13.456% (18.7%)	13.4% (18.4%)	13.8% (20.7%)
Current	M1-THDI	0.341%	0.4% (14.8%)	0.667% (48.9%)	0.44% (22.5%)	0.47% (27.5%)	0.378% (9.8%)
	M5-h11I	11.411%	13.184% (13.4%)	13.01% (12.3%)	11.43% (0.2%)	11.67% (2.2%)	11.43% (0.2%)
	M3-h13I	11.516%	13.049% (11.7%)	11.64% (1.1%)	13.42% (14.2%)	13.06% (11.8%)	13.26% (13.2%)

TABLE 11. Result comparison for wind PMSG-PV model – voltage harmonics.

Forecasting Models	THDV		h11		h13	
	RMSE (%)	MAE (%)	RMSE (%)	MAE (%)	RMSE (%)	MAE (%)
Model-1[1]	3.93%	2.61%	9.61%	7.05%	16.26%	8.72%
Model-2[1]	3.96%	2.65%	9.93%	7.29%	13.67%	6.58%
Model-3[1]	*3.95%*	*2.65%*	*9.38%*	*6.84%*	15.23%	7.57%
Model-4[1]	4.61%	3.56%	9.39%	6.86%	14.62%	7.58%
Model-5[1]	4.74%	3.72%	9.41%	6.93%	14.68%	7.66%
Model-6[1]	4.66%	3.61%	9.35%	6.85%	*14.61%*	*7.56%*
CRNNL[2]	5.91%	4.29%	11.38%	8.83%	19.24%	13.47%
CRNNG[2]	5.58%	4.09%	11.35%	8.80%	20.20%	14.49%
CRNNGL[2]	5.29%	3.89%	11.41%	8.88%	20.04%	14.09%
ANFIS[3]	3.96%	2.80%	9.50%	6.82%	14.71%	7.67%
LSTM[4]	5.40%	3.95%	11.50%	8.08%	13.84%	6.63%

[1] Proposed Models
[2] Publication [23], [24] & [25]
[3] Publication [26]
[4] Publication [27]

the wind PMSG-PV model. LSTM and ANFIS approaches produce good results overall, as can be seen by comparing its performance to that of other models, however proposed hybrid models, which combine ANFIS and ANN models, have an edge.

It has been demonstrated that LSTM and ANFIS both function well on their own. It can also be seen that all models for forecasting Wind PMSG-PV voltage harmonics have given accurate results for all three projected parameters (THDV, h11 and h13). However, the six suggested hybrid models outperform each of the individual models employed by other authors when forecasted separately. It serves as an example of the advantages of using hybrid models. Lastly, the second-best results have been produced by model 3 for THDV and h11 and model 6 for h13 voltage harmonics respectively.

2) CURRENT HARMONICS

Table 12 presents a comparative analysis of the six proposed forecasting models for wind DFIG-PV generator model for current harmonics for the purpose of comparing results.

TABLE 12. Result comparison for wind PMSG-PV model – current harmonics.

Forecasting Models	THDV		h11		h13	
	RMSE (%)	MAE (%)	RMSE (%)	MAE (%)	RMSE (%)	MAE (%)
Model-1[1]	6.93%	0.96%	8.57%	6.38%	15.62%	9.32%
Model-2[1]	*6.92%*	*0.95%*	8.97%	6.74%	15.97%	9.31%
Model-3[1]	6.91%	0.94%	9.06%	6.81%	15.42%	8.94%
Model-4[1]	6.99%	1.39%	*7.62%*	*5.57%*	15.03%	9.50%
Model-5[1]	7.00%	1.39%	7.65%	5.59%	14.97%	9.45%
Model-6[1]	6.99%	1.38%	7.61%	5.56%	*14.97%*	*9.59%*
CRNNL[2]	7.15%	1.66%	20.19%	14.42%	19.83%	7.66%
CRNNG[2]	7.14%	1.66%	9.97%	7.80%	20.53%	14.90%
CRNNGL[2]	7.14%	1.67%	9.93%	7.73%	20.52%	14.63%
ANFIS[3]	6.91%	0.93%	7.67%	5.46%	15.09%	9.75%
LSTM[4]	6.87%	0.81%	11.01%	8.36%	16.16%	7.71%

[1] Proposed Models
[2] Publication [23], [24] & [25]
[3] Publication [26]
[4] Publication [27]

Following the data shown in Table 12, it can be concurred that model 3 delivers accurate results for THDI with RMSE 6.91% and MAE 0.94% for the current harmonics forecast. It should be noted that none of the forecasting methods either the proposed ones in this work or those adopted from other authors have produced accurate prediction results for the THDI parameter. Model 6 performs best for current h11 forecasting, outperforming the other 10 models used to forecast with lowest RMSE (7.61%). For the thirteenth harmonics, Model 5 produces the lowest RMSE (14.97%) and MAE (9.45%).

It is also observed that the second-best result producing models are model 2, model 4 and model 6 for THDI, h11 and h13 current harmonics respectively. Moreover, with the results presented in Table 10, it can be concluded once more that adopting hybrid models has an advantage over employing individual methods as they yield better results overall.

3) RESULT SUMMARY – WIND PMSG-PV MODEL

Model-3 had the best THDV performance for voltage, while model-4 and model-2 outperformed other models for h11 and h13, respectively. With respect to current harmonics, Model-1, model-5, and model-3 were the most reliable for predicting THDI, h11, and h13 respectively. Table 13 provides a summary of the forecasting performance index RMSE for the best performing forecasting models and presents the RMSE and percentage improvement of forecasting results produced by the best performing hybrid models over the other forecasting models utilized in literature for Wind PMSG-PV models. The results presented in Table 13 indicate that

TABLE 13. Best forecast for PMSG-PV model.

	Best Models	RMSE (%)	RMSE (% Improvement)				
			LSTM	ANFIS	CRNNL	CRNNG	CRNNGL
Voltage	M1-THDV	3.936%	5.403% (27.2%)	3.968% (0.8%)	5.913% (33.4%)	5.583% (29.5%)	5.298% (25.7%)
	M6-h11V	9.350%	11.508% (18.8%)	9.49% (1.5%)	11.386% (17.9%)	11.351% (17.6%)	11.414% (18.1%)
	M2-h13V	13.671%	13.842% (1.2%)	14.709% (7.1%)	19.245% (29.0%)	20.2% (32.3%)	20.04% (31.8%)
Current	M3-THDI	6.901%	6.972% (1.0%)	7.18% (3.9%)	7.15% (3.5%)	7.145% (3.4%)	7.149% (3.5%)
	M6-h11I	7.616%	11.013% (30.8%)	7.97% (4.4%)	20.193% (62.3%)	9.974% (23.6%)	9.931% (23.3%)
	M5-h13I	14.971%	16.16% (7.4%)	15.09% (0.8%)	19.83% (24.5%)	20.53% (27.1%)	20.52% (27.0%)

for model-3, voltage THD outperforms the LSTM forecast and offers an improvement of 27.2%. Furthermore, the same hybrid model-3 with respect to RMSE improves results by 0.8% over ANFIS, and 33.4%, 29.5% and 25.7% over CNNRL, CNNRG and CNNRGL respectively.

F. SUMMARY

The comparisons presented in this section concur that, model-1 has been the best performing model for 3 cases (i.e., current THD and h11 for wind DFIG-PV and voltage THD for wind PMSG-PV. Model-2 produced the best performance for 2 cases (voltage h13 forecast for both generator models) and second-best for one case (current THD for wind PMSG-PV). Model-3 has produced accurate results more consistently as compared to other proposed hybrid models as it has yielded the most accurate results for 3 cases (voltage THD and current h13 for wind DFIG-PV and current THD for wind PMSG-PV), and second-best results for 3 cases (h13 for wind DFIG-PV, voltage THD and h11 for wind PMSG-PV). Furthermore, model-4 generated best results for voltage h11 wind DFIG-PV and second-best for current h11 wind PMSG-PV, model-5 performed best for current h13 wind PMSG-PV. Lastly, the performance of model-6 has also been noteworthy as it has produced best results for current h11 wind PMSG-PV generator model and the second-best results for 7 cases (i.e., voltage THD, h11 and current harmonics THD, h11, h13 for wind DFIG-PV and h13 both voltage and current harmonics for wind PMSG-PV model).

With these findings it can be determined that the use of hybrid models proved to be fruitful when the best performing model is considered. Model 3 which is composed of 3LCRN-NGL and ANFIS in first and second stage of its design and Model 6 as vice versa can be categorized as better and more consistent as compared to the other proposed hybrid models. It is also noteworthy that the performance of proposed models was also compared to individual models utilized in other publications [23], [24], [25], [26], and [27]. The best performing models among the six proposed ones in this work proved to be better performing.

IX. CONCLUSION

Harmonics forecasting is one of many methods used to provide inputs while designing harmonics mitigation devices in order to lower harmonics in RES. Use of two hybrid generator models (Wind DFIG-PV and Wind PMSG-PV) was made to generate voltage and current waveforms and extract harmonics from the wind speed and solar irradiation data that represents a real-world response. As a result, the dominant harmonics (h11 & h13) and variations in the voltage and current total harmonics distortions were identified as the predictor variables.

Six hybrid forecasting models were proposed to produce forecasts of the simulated data and the results were validated by comparing the forecasting outputs of the hybrid models proposed in this work with the forecasting techniques used by other authors in the literature. According to the findings that were provided, the best performing hybrid models proposed in this work outperformed the models that are adopted in literature and were used to predict the same data and parameters. The results produced by Model-3 and Model-6 have been established the standout among all models tested, the major limitation of using this approach is the inconsistency to produce results as there has not been a single model that is consistently best performing for all cases tested. It is recommended to apply these two models (models 3 & 6) in different scenarios to further this research.

Referring to the objective of this work, hybrid forecasting models combining the ANN and ANFIS techniques have been achieved with satisfying results as stated. The accuracy, however, needs to be improved and the model performance need to be consistent. More work is required to test these models in different scenarios and circumstances. Since two renewable hybrid generators were utilized to generate harmonics using real world data for Halifax-NS, Canada, it is recommended to use same approach with different geographical locations to test the adaptability and reliability of the proposed forecasting models.

Furthermore, research is required to be carried out in this area to discover other combinations of hybrid models combining other forecasting techniques to achieve improved accuracy.

REFERENCES

[1] P. F. Keebler, "Meshing power quality and electromagnetic compatibility for tomorrow's smart grid," *IEEE Electromagn. Compat. Mag.*, vol. 1, no. 2, pp. 100–103, 2nd Quart., 2012.

[2] H. Hamed and H. Aly, "An intelligent hybrid model of neuro Wavelet, time series and Recurrent Kalman Filter for wind speed forecasting," *J. Sustain. Energy Technol. Assessments*, vol. 41, Oct. 2020, Art. no. 100802, doi: 10.1016/j.seta.2020.100802.

[3] F. Alhaddad, H. H. Aly, and M. El-Hawary, "An overview of active power filters for harmonics mitigation of renewable energies resources," in *Proc. IEEE 10th Annu. Inf. Technol., Electron. Mobile Commun. Conf. (IEMCON)*, Vancouver, BC, Canada, Oct. 2019, pp. 386–393.

[4] F. M. Al Hadi, H. H. Aly, and T. Little, "Harmonics forecasting of wind and solar hybrid model driven by DFIG and PMSG using ANN and ANFIS," *IEEE Access*, vol. 11, pp. 55413–55424, 2023.

[5] F. Al Hadi, H. H. H. Aly, and T. Little, "Harmonics prediction and mitigation using adaptive neuro fuzzy inference system model based on hybrid of wind solar driven by DFIG," in *Proc. IEEE 13th Annu. Inf. Technol., Electron. Mobile Commun. Conf. (IEMCON)*, Oct. 2022, pp. 338–342.

[6] F. A. Hadi, H. H. H. Aly, and T. Little, "A proposed adaptive filter for harmonics mitigation based on adaptive neuro fuzzy inference system model for hybrid wind solar energy system," in *Proc. IEEE Can. Conf. Electr. Comput. Eng. (CCECE)*, Sep. 2022, pp. 165–169.

[7] *IEEE Recommended Practice and Requirements for Harmonics Control in Electric Power Systems*, Standard IEEE Std 519-2014, Revision of IEEE Std 519-1992, 2014, pp. 1–29.
[8] *Limits for Harmonics Current Emissions (Equipment Input Current< 16 A Per Phase)*, Standard IEC 61000-3-2, International Electrotechnical Commission, London, U.K., 2005.
[9] *Limitation of Emission of Harmonics Currents in Low- Voltage Power Supply System's Equipment With Rated Current Greater Than 16 A*, Standard IEC 61000-3-4, 1998.
[10] *General Guide on Harmonics and Inter-Harmonics Measurements and Instrumentation for Power Supply and Equipment Connected Thereto*, Standard IEC 61000-4-7, International Electrotechnical Commission, London, U.K., 2002.
[11] S. K. Jain and S. N. Singh, "Harmonics estimation in emerging power system: Key issues and challenges," *Electr. Power Syst. Res.*, vol. 81, no. 9, pp. 1754–1766, Sep. 2011.
[12] T. Ortmeyer and K. Chakravarthi, "The effects of power system harmonics on power system equipment and loads," *IEEE Trans. Power Appar. Syst.*, vol. PAS-104, no. 9, pp. 2555–2563, Sep. 1985.
[13] V. E. Wagner, J. C. Balda, D. C. Griffith, A. McEachern, T. M. Barnes, D. P. Hartmann, D. J. Phileggi, A. E. Emannuel, W. F. Horton, W. E. Reid, R. J. Ferraro, and W. T. Jewell, "Effects of harmonics on equipment," *IEEE Trans. Power Del.*, vol. 8, no. 2, pp. 672–680, Apr. 1993.
[14] A. B. Nassif, W. Xu, and W. Freitas, "An investigation on the selection of filter topologies for passive filter applications," *IEEE Trans. Power Del.*, vol. 24, no. 3, pp. 1710–1718, Jul. 2009.
[15] D. Bohaichuk, C. Muskens, and W. Xu, "Mitigation of harmonics in oil field electric systems using a centralized medium voltage filter," in *Proc. 9th Int. Conf. Harmon. Quality Power.*, 2000, pp. 614–618.
[16] C.-J. Chou, C.-W. Liu, J.-Y. Lee, and K.-D. Lee, "Optimal planning of large passive-harmonic-filters set at high voltage level," *IEEE Trans. Power Syst.*, vol. 15, no. 1, pp. 433–441, Feb. 2000.
[17] A. S. Yilmaz, A. Alkan, and M. H. Asyali, "Applications of parametric spectral estimation methods on detection of power system harmonics," *Electr. Power Syst. Res.*, vol. 78, no. 4, pp. 683–693, Apr. 2008.
[18] A. Yazdani and R. Iravani, *Voltage-Sourced Converters in Power Systems: Modeling, Control, and Applications*. Hoboken, NJ, USA: Wiley, 2010.
[19] N. Mohan, T. M. Undeland, and W. P. Robbins, *Power Electronics: Converters, Applications, and Design*. Hoboken, NJ, USA: Wiley, 2003.
[20] P. K. Ray, P. S. Puhan, and G. Panda, "Real time harmonics estimation of distorted power system signal," *Int. J. Electr. Power Energy Syst.*, vol. 75, pp. 91–98, Feb. 2016.
[21] P. Ivry, O. Oke, D. W. Thomas, and M. Sumner, "Predicting harmonics distortion of multiple converters in a power system," *J. Electr. Comput. Eng.*, vol. 2017, Jun. 2017, Art. no. 7621413.
[22] M. M. H. Alhaj, N. M. Nor, V. S. Asirvadam, and M. F. Abdullah, "Comparison of power system harmonics prediction," *Proc. Technol.*, vol. 11, pp. 628–634, Jan. 2013.
[23] P. Rodríguez-Pajarón, A. Hernández Bayo, and J. V. Milanović, "Forecasting voltage harmonic distortion in residential distribution networks using smart meter data," *Int. J. Electr. Power Energy Syst.*, vol. 136, Mar. 2022, Art. no. 107653.
[24] H. Mori and S. Suga, "Power system harmonics prediction with an artificial neural network," in *Proc. IEEE. Int. Symp. Circuits Syst.*, Jun. 1991, pp. 1129–1132.
[25] M. Žnidarec, Z. Klaić, D. Šljivac, and B. Dumnić, "Harmonic distortion prediction model of a grid-tie photovoltaic inverter using an artificial neural network," *Energies*, vol. 12, no. 5, p. 790, Feb. 2019.
[26] M. Panoiu, C. Panoiu, and L. Ghiormez, "Neuro-fuzzy modeling and prediction of current total harmonic distortion for high power nonlinear loads," in *Proc. Innov. Intell. Syst. Appl. (INISTA)*, Jul. 2018, pp. 1–7.
[27] L. Shengqing, Z. Huanyue, X. Wenxiang, and L. Weizhou, "A harmonic current forecasting method for microgrid HAPF based on the EMD-SVR theory," in *Proc. 3rd Int. Conf. Intell. Syst. Design Eng. Appl.*, Jan. 2013, pp. 70–72.
[28] E. M. Kuyunani, A. N. Hasan, and T. Shongwe, "Improving voltage harmonics forecasting at a wind farm using deep learning techniques," in *Proc. IEEE 30th Int. Symp. Ind. Electron. (ISIE)*, Jun. 2021, pp. 1–6.
[29] A. Y. Hatata and M. Eladawy, "Prediction of the true harmonic current contribution of nonlinear loads using NARX neural network," *Alexandria Eng. J.*, vol. 57, no. 3, pp. 1509–1518, Sep. 2018.
[30] Y. Pang, "Short-term harmonic forecasting and evaluation affected by electrified railways on the power grid based on stack auto encoder neural network method and the comparison to BP method," in *Proc. 13th IEEE Conf. Ind. Electron. Appl. (ICIEA)*, Jun. 2018, pp. 1159–1165.
[31] H. H. H. Aly, "A novel approach for harmonic tidal currents constitutions forecasting using hybrid intelligent models based on clustering methodologies," *Renew. Energy*, vol. 147, pp. 1554–1564, Mar. 2020, doi: 10.1016/j.renene.2019.09.107.
[32] MATLAB Simulink. *Wind Farm—DFIG Detailed Model*. Accessed Sep. 18, 2022.
[33] *DATASET Typical Meteorological Data Access Service*, Accessed: Apr. 30, 2022.
[34] *MODEL Detailed Modelling of A 1.5MW Wind Turbine Based On Direct-Driven PMSG*. Accessed: Jan. 23, 2020.
[35] W. S. McCulloch and W. Pitts, "A logical calculus of ideas immanent in nervous activity," *Bull. Math. Biophys.*, vol. 5, no. 4, pp. 115–133, Dec. 1943.
[36] H. H. H. Aly, "A hybrid optimized model of adaptive neuro-fuzzy inference system, recurrent Kalman filter and neuro-wavelet for wind power forecasting driven by DFIG," *Energy*, vol. 239, Jan. 2022, Art. no. 122367.
[37] D. R. Baughman and Y. A. Liu, "Fundamental and practical aspects of neural computing," in *Neural Networks in Bioprocessing and Chemical Engineering*. 1995, pp. 21–109.
[38] H. H. H. Aly, "A proposed intelligent short-term load forecasting hybrid models of ANN, WNN and KF based on clustering techniques for smart grid," *Electr. Power Syst. Res.*, vol. 182, May 2020, Art. no. 106191.
[39] H. Aly, "Forecasting, modeling and control of tidal currents electrical energy systems," Ph.D. dissertation, Dept. Elect. Comput. Eng., Dalhousie Univ., Halifax, NS, Canada, 2012.
[40] R. R. Yager and D. P. Filev, "Generation of fuzzy rules by mountain clustering," *J. Intell. Fuzzy Syst.*, vol. 2, no. 3, pp. 209–219, 1994.
[41] H. H. H. Aly, "A novel deep learning intelligent clustered hybrid models for wind speed and power forecasting," *Energy*, vol. 213, Dec. 2020, Art. no. 118773, doi: 10.1016/j.energy.2020.118773.

FAWAZ M. AL HADI received the B.Sc. degree in electrical engineering from the Riyadh College of Technology, Saudi Arabia, in 2007, and the M.Sc. degree from Dalhousie University, in 2014, where he is currently pursuing the Ph.D. degree in electrical and computer engineering. His research interest includes renewable energy integration.

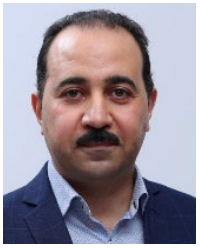

HAMED H. ALY (Senior Member, IEEE) received the B.Eng. and MASc degrees (Hons.) in electrical engineering from Zagazig University, Egypt, in 1999 and 2005, respectively, and the Ph.D. degree from Dalhousie University, Canada, in 2012. He was a Postdoctoral Research Associate for one year and an Instructor for three years with Dalhousie University. He was with Acadia University, as an Assistant Professor, for three years. He is currently an Assistant Professor with Dalhousie University. His research interests include micro grids, smart grids, distributed generation, power quality issues, applications of artificial intelligence in power systems, energy management, green energy, and optimization.

TIMOTHY LITTLE is currently the Associate Dean of the Faculty of Engineering and a full-time Associate Professor with the Department of Electrical and Computer Engineering, Dalhousie University, Canada. His research interests include engineering education, wind energy and renewable generation, power electronics, and electromechanical energy conversion.